World Journal of

Stem Cells

WJSC World Journal of Stem Cells

ORIGINAL ARTICLE

Basic Study

Contents

ABOUT COVER

Editorial Board Member of *World Journal of Stem Cells*, Khawaja Husnain Haider, PhD, Professor, Department of Basic Sciences, Sulaiman Al-Rajhi University (SRU), Al-Qaseem 52726, Saudi Arabia. kh.haider@gmail.com

AIMS AND SCOPE

The primary aim of *World Journal of Stem Cells* (*WJSC*, *World J Stem Cells*) is to provide scholars and readers from various fields of stem cells with a platform to publish high-quality basic and clinical research articles and communicate their research findings online. *WJSC* publishes articles reporting research results obtained in the field of stem cell biology and regenerative medicine, related to the wide range of stem cells including embryonic stem cells, germline stem cells, tissue-specific stem cells, adult stem cells, mesenchymal stromal cells, induced pluripotent stem cells, embryonal carcinoma stem cells, hemangioblasts, lymphoid progenitor cells, *etc*.

INDEXING/ABSTRACTING

The *WJSC* is now abstracted and indexed in Science Citation Index Expanded (SCIE, also known as SciSearch®), Journal Citation Reports/Science Edition, PubMed, PubMed Central, Scopus, Biological Abstracts, BIOSIS Previews, Reference Citation Analysis, China National Knowledge Infrastructure, China Science and Technology Journal Database, and Superstar Journals Database. The 2023 Edition of Journal Citation Reports® cites the 2022 impact factor (IF) for *WJSC* as 4.1; IF without journal self cites: 3.9; 5-year IF: 4.5; Journal Citation Indicator: 0.53; Ranking: 15 among 29 journals in cell and tissue engineering; Quartile category: Q3; Ranking: 99 among 191 journals in cell biology; and Quartile category: Q3. The *WJSC*'s CiteScore for 2022 is 8.0 and Scopus CiteScore rank 2022: Histology is 9/57; Genetics is 68/325; Genetics (clinical) is 19/90; Molecular Biology is 119/380; Cell Biology is 95/274.

RESPONSIBLE EDITORS FOR THIS ISSUE

Production Editor: *Xiang-Di Zhang*; **Production Department Director:** *Xu Guo*; **Editorial Office Director:** *Jia-Ru Fan*.

ORIGINAL ARTICLE

Basic Study

Interferon-γ priming enhances the therapeutic effects of menstrual blood-derived stromal cells in a mouse liver ischemia-reperfusion model

Qi Zhang, Si-Ning Zhou, Jia-Min Fu, Li-Jun Chen, Yang-Xin Fang, Zhen-Yu Xu, Hui-Kang Xu, Yin Yuan, Yu-Qi Huang, Ning Zhang, Yi-Fei Li, Charlie Xiang

Qi Zhang, Si-Ning Zhou, Jia-Min Fu, Li-Jun Chen, Yang-Xin Fang, Hui-Kang Xu, Yin Yuan, Yu-Qi Huang, Ning Zhang, Yi-Fei Li, State Key Laboratory for Diagnosis and Treatment of Infectious Diseases, National Clinical Research Center for Infectious Diseases, National Medical Center for Infectious Diseases, Collaborative Innovation Center for Diagnosis and Treatment of Infectious Diseases, The First Affiliated Hospital, Zhejiang University School of Medicine, Hangzhou 310003, Zhejiang Province, China

Qi Zhang, Si-Ning Zhou, Jia-Min Fu, Li-Jun Chen, Yang-Xin Fang, Hui-Kang Xu, Yin Yuan, Yu-Qi Huang, Ning Zhang, Yi-Fei Li, Research Units of Infectious Disease and Microecology, Chinese Academy of Medical Sciences, Hangzhou 310003, Zhejiang Province, China

Zhen-Yu Xu, Innovative Precision Medicine Group, Shulan Hospital, Hangzhou 311215, Zhejiang Province, China

Charlie Xiang, The First Affiliated Hospital, Zhejiang University School of Medicine, Hangzhou 310003, Zhejiang Province, China

Corresponding author: Charlie Xiang, PhD, Director, Professor, The First Affiliated Hospital, Zhejiang University School of Medicine, No. 79 Qingchun Road, Hangzhou 310003, Zhejiang Province, China. cxiang@zju.edu.cn

Abstract

BACKGROUND

Mesenchymal stem cells (MSCs) have been used in liver transplantation and have certain effects in alleviating liver ischemia-reperfusion injury (IRI) and regulating immune rejection. However, some studies have indicated that the effects of MSCs are not very significant. Therefore, approaches that enable MSCs to exert significant and stable therapeutic effects are worth further study.

AIM

To enhance the therapeutic potential of human menstrual blood-derived stromal cells (MenSCs) in the mouse liver ischemia-reperfusion (I/R) model *via* interferon-γ (IFN-γ) priming.

METHODS

Apoptosis was analyzed by flow cytometry to evaluate the safety of IFN-γ priming, and indoleamine 2,3-dioxygenase (IDO) levels were measured by quantitative real-time reverse transcription polymerase chain reaction, western blotting, and ELISA to evaluate the efficacy of IFN-γ priming. *In vivo*, the liver I/R model was established in male C57/BL mice, hematoxylin and eosin and TUNEL staining was performed and serum liver enzyme levels were measured to assess the degree of liver injury, and regulatory T cell (Treg) numbers in spleens were determined by flow cytometry to assess immune tolerance potential. Metabolomics analysis was conducted to elucidate the potential mechanism underlying the regulatory effects of primed MenSCs. *In vitro*, we established a hypoxia/reoxygenation (H/R) model and analyzed apoptosis by flow cytometry to investigate the mechanism through which primed MenSCs inhibit apoptosis. Transmission electron microscopy, western blotting, and immunofluorescence were used to analyze autophagy levels.

RESULTS
IFN-γ-primed MenSCs secreted higher levels of IDO, attenuated liver injury, and increased Treg numbers in the mouse spleens to greater degrees than untreated MenSCs. Metabolomics and autophagy analyses proved that primed MenSCs more strongly induced autophagy in the mouse livers. In the H/R model, autophagy inhibitors increased the level of H/R-induced apoptosis, indicating that autophagy exerted protective effects. In addition, primed MenSCs decreased the level of H/R-induced apoptosis *via* IDO and autophagy. Further rescue experiments proved that IDO enhanced the protective autophagy by inhibiting the mammalian target of rapamycin (mTOR) pathway and activating the AMPK pathway.

CONCLUSION
IFN-γ-primed MenSCs exerted better therapeutic effects in the liver I/R model by secreting higher IDO levels. MenSCs and IDO activated the AMPK-mTOR-autophagy axis to reduce IRI, and IDO increased Treg numbers in the spleen and enhanced the MenSC-mediated induction of immune tolerance. Our study suggests that IFN-γ-primed MenSCs may be a novel and superior MSC product for liver transplantation in the future.

Key Words: Mesenchymal stem cells; Cell therapy; Reperfusion injury; T-lymphocytes; Autophagy; Liver

Core Tip: In this study, we identified a suitable interferon-γ (IFN-γ) priming strategy for menstrual blood-derived stromal cells (MenSCs) in the liver ischemia-reperfusion (I/R) model and proved that primed MenSCs could significantly increase the number of regulatory cells in the spleen by secreting higher levels of indoleamine 2,3- dioxygenase (IDO) and thereby exhibited better immunoregulatory potential. Besides, through metabolomics and related molecular biology experiments, we found that IDO could reduce ischemia-reperfusion injury *via* the AMPK-mammalian target of rapamycin-autophagy axis. Our study suggests that IFN-γ-primed MenSCs may be a novel and superior mesenchymal stem cell product for liver transplantation in the future.

INTRODUCTION

Liver transplantation is the only therapeutic option that is available to patients with terminal liver failure. Both liver ischemia-reperfusion injury (IRI), which occurs during surgery, and immune rejection, which occurs after surgery, affect the results of liver transplantation[1]. Therefore, there is an urgent need to develop effective strategies for treating IRI and immune rejection.

Mesenchymal stem cells (MSCs) have been used in liver transplantation and have shown certain therapeutic effects[2-4]. For example, MSCs alleviated hepatocellular apoptosis in a mouse liver ischemia-reperfusion (I/R) model *via* PINK1-dependent mitophagy[5]. In a clinical study, the percentage of regulatory T cells (Tregs) and the ratio of Tregs to T helper 17 (Th17) cells, which can be used as indicators of immune tolerance potential, were significantly increased in liver transplant recipients 4 wk after MSC infusion[6]. However, the results of another clinical study showed that the infusion of MSCs into liver transplant recipients before surgery was safe, but only mild changes in the peripheral blood immunoregulatory T cell numbers and natural killer cell numbers were observed in these patients[7]. In addition, the administration of immunosuppressive agents with MSCs showed no synergistic effect compared with the administration of immunosuppressive agents alone in a rat liver transplant study[8]. Therefore, approaches that enable MSCs to exert

more significant protective effects in reducing IRI and inducing immune tolerance in liver transplantation deserve further study.

Priming can induce an anti-inflammatory state in MSCs, causing them to secrete more bioactive molecules and improving their therapeutic effects[9,10]. Interferon (IFN)-γ-primed MSCs have been shown to have more stable and stronger abilities to regulate immune responses and prevent damage in many disease models[11-13]. Priming with IFN-γ increases the mRNA expression of Toll-like receptor 3 and the secretion of immunosuppressive molecules, such as indoleamine 2,3-dioxygenase (IDO), interleukin (IL)-10, hepatocyte growth factor, and kynurenine[14]. IDO, an enzyme involved in tryptophan metabolism, has been widely reported to regulate T-cell immunity, specifically by promoting the differentiation of Tregs, inhibiting Th17 cells, and promoting immune tolerance and immune escape[15,16]. Additionally, compared with control conditions, IFN-γ priming significantly induces IDO expression, enhances the immunoregulatory effect of MSCs on T cells, increases Treg differentiation, and promotes immune tolerance[17].

Menstrual blood-derived stromal cells (MenSCs) have been studied in several clinical and preclinical trials, and their safety and immunomodulatory properties have been fully demonstrated[18-20]. In addition, MenSCs can be collected in a manner that is painless, noninvasive, convenient, and inexpensive, thus, their use in cell-based therapy has high clinical and economic value. In this study, we hypothesized that IFN-γ-primed MenSCs could secrete higher levels of IDO to better induce immune tolerance in a mouse liver I/R model. However, whether priming with IFN-γ affects the viability of MenSCs themselves is unclear. Moreover, whether IFN-γ-primed MenSCs, which represent a new type of modified MSC product, can better mitigate liver injury in the liver I/R model has not been clarified. Therefore, it is worthwhile to further study appropriate priming strategies and whether primed MenSCs can exert better therapeutic effects in the liver I/R model.

MATERIALS AND METHODS

MenSCs

MenSCs were provided by the Innovative Precision Medicine Group (IPM, Hangzhou, China) and cultured as described in our previous study[2-4]. Briefly, the cells were cultured in α-minimum essential medium (Thermo Fisher Scientific, United States) supplemented with 10% foetal bovine serum (FBS) (Thermo Fisher Scientific, United States) and 1% penicillin-streptomycin solution (Thermo Fisher Scientific, United States) in an incubator at 37 °C with 5% CO_2. When the cells reached 80%-90% confluence, they were subcultured with 0.25% trypsin-EDTA (Thermo Fisher Scientific) and passaged 5-8 times before being used in experiments. MenSCs were identified based on their surface marker expression and differentiation potential.

Flow cytometry was performed to detect the surface markers of MenSCs. The cells were collected, washed twice with staining buffer (BD, Biosciences, San Jose, CA), and incubated with antibodies against CD29, CD34, CD45, CD73, CD90, CD105, CD117, and human leukocyte antigen-DR (HLA-DR) (PE, BD, Biosciences, San Jose, United States) at 4 °C for 30 min in the dark. Negative controls (NCs) were established with the corresponding isotype control antibodies. A flow cytometer (ACEA Biosciences, CA, United States) was used to analyze all the cells.

Osteogenic, adipogenic, and chondrogenic differentiation was induced to evaluate the multi-differentiation potential of the cells. Briefly, approximately 5×10^5 MenSCs were cultured in 6-well plates for 3-4 wk with osteogenic differentiation medium (Cyagen Biosciences, United States) or adipogenic differentiation medium (Cyagen Biosciences, United States) in an incubator at 37 °C with 5% CO_2 to promote osteogenic or adipogenic differentiation, respectively; the medium was changed every 1-3 d according to the instructions. After fixation with 4% formaldehyde, the cells were incubated with Alizarin Red or Oil Red O solution for 30 min to label calcium or neutral lipids, respectively. Chondrogenic differentiation was performed in a 15 mL centrifuge tube. Approximately 5×10^5 MenSCs were centrifuged and cultured with 1 mL of human MSC chondrogenic differentiation medium (Cyagen Biosciences, United States) in an incubator at 37 °C with 5% CO_2 for 3-4 wk; the medium was changed every 2-3 d according to the instructions. After fixation with 4% formaldehyde, the pelleted cells were embedded in paraffin, cut into 4 mm sections, and stained with Alcian blue solution to label cartilage.

Priming of MenSCs and IDO quantification

IFN-γ (Miltenyi Biotec Inc., Auburn, CA, United States) at a concentration of 100 or 200 ng/mL was used to prim MenSCs for 24, 48, or 72 h. After the cells were collected, RNA or protein was extracted to measure IDO expression by quantitative real-time reverse transcription polymerase chain reaction (qRT-PCR) or western blotting assays, respectively, as described below. Additionally, the supernatants were collected to evaluate the release of IDO using a Human IDO ELISA Kit (Sangon Biotech, Shanghai, China).

Establishment of the mouse liver I/R model and animal grouping

Six- to eight-week-old male C57BL/6J mice (Slac Laboratory Animal Corporation, Shanghai, China) were housed in a specific pathogen-free room (23 ± 2 °C, 12 h light/12 h dark cycle, and 50% humidity) at the Laboratory Animal Center of Zhejiang University with plenty of food and water for two weeks prior to experimentation. All the procedures used for the animal experiments, the number of animals, and the ethics of the animal housing environment were performed according to the 3Rs rule and approved by the Experimental Animal Center of Zhejiang University, and the ethical approval number is ZJU20210299.

Anesthesia: Before all the surgical procedures, 1% pentobarbital sodium (100 µL/10 g intraperitoneal injection) was used to anesthetize the mice (weight 20-23 g)[5]. Surgical procedure: All the mice received a ventral midline incision. Hepatic arteries, portal veins, and bile ducts were clipped with an atraumatic vascular clip to interrupt 70% of the blood supply to the liver. After 1 h of ischemia, the atraumatic vascular clamps were removed to terminate the ischemia; the wounds were sutured layer by layer, and erythromycin ointment was applied to prevent infection. The mice were resuscitated on a 37 °C blanket to maintain their body temperature. Group design: The sample size (total n = 27, and n = 3/group), grouping, and animal experiment schedule were decided based on a similar study published previously[2] and can be found in Figure 1. To establish the short-term I/R model, the mice were randomly divided into the sham group, IR group, IRM group, and IRM (IFN-γ) group (n = 3/group). The model mice in the IR, IRM, and IRM (IFN-γ) groups were administered 100 µL of phosphate buffered saline (PBS) or MenSCs (10^6/100 µL intravenous injection) or IFN-γ-primed MenSCs (10^6/100 µL intravenous injection) 1 h before the surgery. The mice in the sham group received only a ventral midline incision and were sutured after injection of PBS. After 6 h of reperfusion, the mice were euthanized in a classic, quick, and painless manner (150 mg/kg pentobarbital sodium, intraperitoneal injection), and tissue samples were collected for further investigation.

To establish the long-term I/R model, the mice were randomly divided into the sham group, IR group, IRM group, IRM (IFN-γ) group, and IRM (IFN-γ) + 1-methyl-D-tryptophan (1MT) group (n = 3/group). The treatment plan was similar to that used for the short-term model, with the exception that 1MT (2 mg/mL; MCE, New Orleans, LA, United States) was added to the drinking water of the mice in the IRM (IFN-γ) + 1MT group, and the mice in this group had continuous access to this supplemented water starting from the day of the surgery (day 0) until the seventh day (day 7). The mice in the other groups were given normal water without 1MT. All the long-term I/R model mice were euthanized (150 mg/kg pentobarbital sodium, intraperitoneal injection) on day 7 for tissue collection.

Assessment of liver injury
The serum alanine aminotransferase (ALT) and aspartate aminotransferase (AST) levels were measured using the ALT Kit and AST Kit (Nanjing Jiancheng Bioengineering Institute, Nanjing, China), respectively, to assess the liver injury. Liver injury was also assessed by hematoxylin and eosin staining. Sections were examined under a microscope, and Suzuki's injury criteria (Supplementary Table 1) were utilized to determine the histological damage score by a researcher who was blinded to the group of the immunohistochemistry sections.

qRT-PCR
To confirm the effects on the transcriptome, RNA was extracted from cells using the RNA Extraction Kit (TaKaRa, Beijing, China). Prime Script TMRT Master Mix and TB Green Premix Ex Taq Bulk (TaKaRa, Beijing, China) were used for qRT-PCR. First, Buffer RL was added to the cells to lyse them, and the lysis solution was transferred to a gDNA Eraser Spin Column to remove impurities and gDNA. Then, 70% ethanol was added to the filtrate, and the mixture was moved to an RNA spin column to capture the RNA. Then, the RNA spin column was cleaned with Buffer RWA and Buffer RWB. The RNA solution was obtained by eluting the RNA with RNase-free dH$_2$O. Then, we mixed an appropriate amount of RNA with 5 × A solution and RNase-free dH$_2$O to a final volume of 10 µL, and reverse transcription was performed to obtain cDNA. Then, the TB Green mix (12.5 µL), forward PCR primer (10 µM × 0.5 µL, Supplementary Table 2), reverse PCR primer (10 µM × 0.5 µL, Supplementary Table 2), DNA template (2 µL), and 9.5 µL ddH$_2$O were mixed in a final volume of 25 µL. The qRT-PCR conditions were as follows: 95 °C for 30 s ; 40 cycles of 95 °C for 5 s and 60 °C for 30 s for 2 step PCR; and 95 °C for 15 s, 60 °C for 30 s, and 95 °C for 15 s for dissociation. The melting curves were determined, and the cycle threshold (CT) values of the β-actin (ACTB) transcripts were used to normalize the CT values of the IDO transcripts. The qRT-PCR data were analyzed using the ΔΔCT method.

Western blotting
Liver tissues and cells were lysed with a moderate amount of lysis buffer, which was composed of radioimmunoprecipitation assay buffer (RIPA Lysis Buffer, 10 ×, Merck KGaA, Darmstadt, Germany), a protease and phosphatase inhibitor cocktail for mammalian cell and tissue extracts (Beyotime, Shang Hai, China) and ddH$_2$O, on ice for 30-60 min. Equal amounts of proteins were subjected to 12% or 8% SDS polyacrylamide gel electrophoresis and then transferred to polyvinylidene difluoride membranes (Millipore, Billerica, MA, United States). The membranes were incubated with 5% nonfat milk for 1 h and then with the primary antibodies overnight at 4 °C; the primary antibodies included antibodies against IDO (16630, Cell Signaling Technology, United States), LC3 (12741, Cell Signaling Technology, United States), AMPKα (total) (5831, Cell Signaling Technology, United States), p-AMPKα (50081, Cell Signaling Technology, United States), mammalian target of rapamycin (mTOR) (total) (2983, Cell Signaling Technology, United States), p-mTOR (5536, Cell Signaling Technology, United States), and β-actin (ACTB) (8227, Abcam, United States). The membranes were then washed three times with Tris-buffered saline with Tween 20 (TBST) and incubated with the secondary antibody [anti-rabbit immunoglobulin G (IgG), Sigma, United States or anti-mouse IgG, Sigma, United States] for 1 h at room temperature. The membranes were washed three times with TBST and visualized by enhanced chemiluminescence with a Fluor Chem Systems imager (Bio-Rad, CA, United States). The intensities of the bands were determined using ImageJ software.

Transmission electron microscopy
Liver samples were cut into 1-mm^3 pieces and fixed with 2.5% glutaraldehyde overnight at 4 °C. After fixation and dehydration, all the samples were stained with osmic acid and uranyl acetate. Then, we used an ultramicrotome to slice the samples and obtain ultrathin sections. All the samples were imaged with a transmission electron microscope (Talos
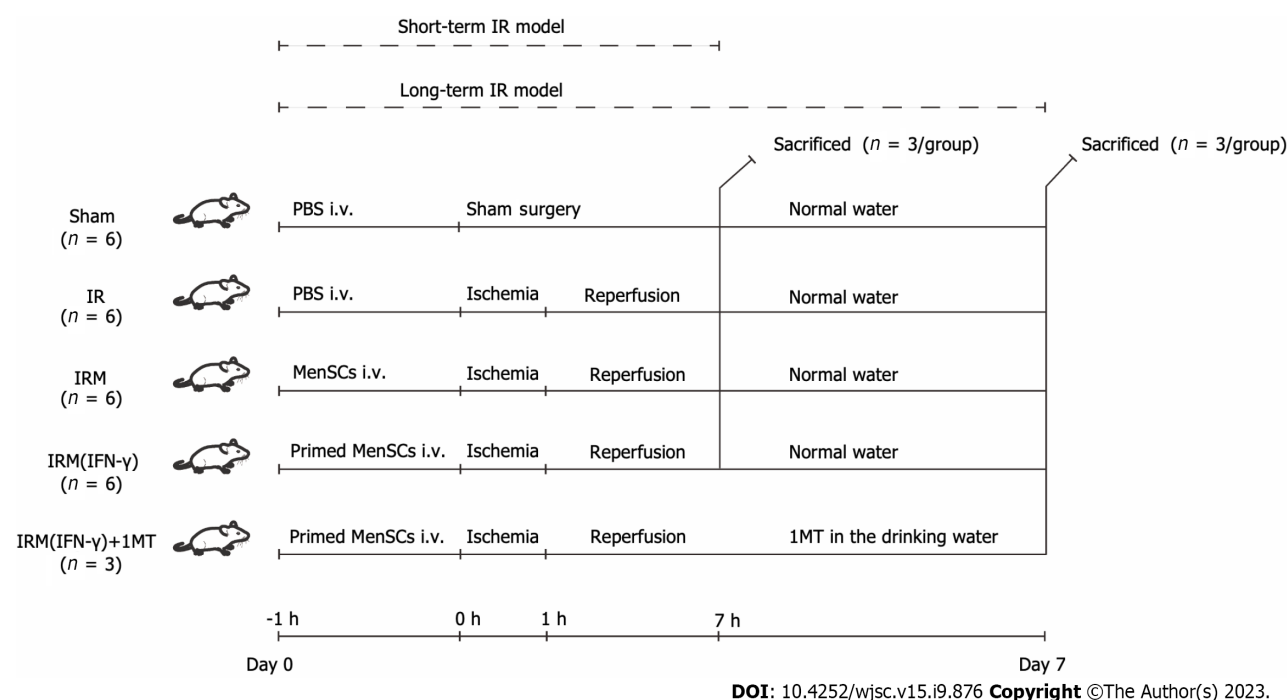
Figure 1 Animal experiment grouping and timeline. Detailed descriptions are provided in the Materials and Methods. In brief, we established short-term and long-term liver ischemia-reperfusion mouse models to explore the therapeutic potential of menstrual blood-derived stromal cells (MenSCs) and primed MenSCs. MenSCs: Menstrual blood-derived stromal cells; IFN-γ: Interferon-γ; 1MT: 1-methyl-D-tryptophan; IR: Ischemia-reperfusion; IRM: Combination treated with ischemia-reperfusion and menstrual blood-derived stromal cells; IRM (IFN-γ): Combination treated with ischemia-reperfusion and interferon-γ-primed menstrual blood-derived stromal cells; PBS: Phosphate buffered saline; i.v.: Intravenous injection.

L120C, Thermo Fisher, Carlsbad, CA, United States) to confirm and monitor autophagy, and the number of autophagic vacuoles in each cell was quantified.

Establishment of the hypoxia/reoxygenation model in L02 cells and grouping

Under normoxic conditions, the L02 cells (FuHeng Biology, Shanghai, China) were cultured in 1640 complete medium (RPMI 1640 medium supplemented with 10% FBS and 1% penicillin-streptomycin) in a typical incubator at 37 °C with 5% CO_2. To simulate liver IRI, the L02 cells were subjected to hypoxia/reoxygenation (H/R). Briefly, after 6 h of culture in FBS-free 1640 medium in a 2.5 L sealed culture tank (MGC, Tokyo, Japan) under hypoxic conditions, the cells were transferred to atypical incubator for 4 h to allow reoxygenation. The hypoxic conditions in the sealed culture tank (94% N_2, 5% CO_2, and 1% O_2) were maintained by AnaeroPack-Anaero-5% (MGC, Tokyo, Japan).

Group design: The cells that were cultured under normal oxygen conditions were divided into the NC group, 3-methyladenine (3MA) group, 1MT group, MenSCs group, and MenSC (IFN-γ) group. The cells that were cultured under H/R conditions were divided into the HR group, HR + 3MA group, HR + 1MT group, HRM group, HRM (IFN-γ) group, HRM (IFN-γ) + 3MA group, and HRM (IFN-γ) + 1MT group.

The NC group consisted of cells cultured in 1640 complete medium without any other treatment. The cells in the 3MA group and 1MT group were cultured in 1640 complete medium with 10 mmol/L 3MA (an autophagy inhibitor, MCE, New Orleans, LA, United States) or 1 mmol/L 1MT (an IDO inhibitor, MCE, New Orleans, LA, United States). The cells in the MenSCs group and MenSC (IFN-γ) group were cocultured with MenSCs or MenSC (IFN-γ), respectively, in 1640 complete medium using a coculture chamber as described previously. The HR group, HR + 3MA group, HR + 1MT group, HRM group, and HRM (IFN-γ) group, were subjected to treatments that were similar to those used in the experiments conducted under normal oxygen conditions, but H/R treatment was added. In addition to the HRM (IFN-γ) treatment, the cells in the HRM (IFN-γ) + 3MA group and HRM (IFN-γ) + 1MT group received 3MA and 1MT in the medium, respectively.

Quantitative GFP-LC3 analysis

L02 cells in every group were transfected with pCMV-GFP-LC3 (Beyotime, Shang Hai, China) for 24 h before treatment. We used a confocal laser scanning microscope (Olympus Corporation, Japan) to detect fluorescence emission. Intense punctate GFP-LC3 aggregates in the nucleus and cytoplasm were considered to indicate autophagy, whereas diffuse distribution of GFP-LC3 was considered to indicate non-autophagic conditions. We counted the number of intense punctate GFP-LC3 aggregates in each cell to indicate the number of autophagosomes.

Treg analysis

The mononuclear cells in the spleen were harvested by gradient centrifugation using Ficoll 1.084 (Cytiva, Logan, UT, United States). FACS was performed with 3 fluorochrome-conjugated antibodies: Anti-CD4 monoclonal antibody (APC,

17-0041-83, eBioscience, CA, United States), anti-CD25 monoclonal antibody (PE, 12-0251-82, eBioscience, CA, United States), and anti-FOXP3monoclonal antibody (FITC, 11-5773-82, eBioscience, CA, United States). Nuclear permeabilization was performed with a FoxP3/transformation factor permeabilization buffer (00-5523-00, eBioscience, CA, United States) before the anti-FoxP3 antibody was added to the cells for incubation. Cell fluorescence was evaluated using a flow cytometer (ACEA Biosciences, CA, United States). The percentage of CD4$^+$ CD25$^+$ cells among all mononuclear cells and the percentage of FoxP3$^+$ cells among the CD4$^+$CD25$^+$ cells were recorded, and the product of these percentages was used to represent the percentage of Tregs among all mononuclear cells.

Statistical analysis

The metabolomics data were analyzed using the free online Majorbio choice platform (cloud.majorbio.com). Other data were analyzed using Prism version 5.0 (GraphPad, United States). The data are shown as the means ± SDs or means ± SEMs. One-way ANOVA was used for comparisons of three or more groups. A *P* value of <0.05 was considered to indicate a significant difference ([a]*P* < 0.05, [b]*P* < 0.01, [c]*P* < 0.001, and [d]*P* < 0.0001), and *P* values ≥ 0.05 were considered to indicate no significant difference (NS).

RESULTS

Characterization of MenSCs

Primary MenSCs were cultured and exhibited adherent growth after approximately 24 h, and obvious cell proliferation was observed as soon as the cells became round and fusiform. According to a phenotypic analysis, MenSCs expressed CD29, CD73, CD90, and CD105, but they did not express CD45, CD80, CD117, or HLA-DR (Figure 2A). Specific staining showed that MenSCs could undergo osteogenic, chondrogenic, and adipogenic lineage differentiation (Figures 2B-D). The MenSCs that were used in this study met the International Society for Cellular Therapy criteria for the definition of multipotent MSCs[21].

MenSC priming with IFN-γ

In this study, we hypothesized that IFN-γ-primed MenSCs could secrete higher levels of IDO to induce stronger immune tolerance in a liver I/R model. Therefore, to determine the appropriate priming strategy, we evaluated the safety and efficacy of priming by measuring the degree of cell apoptosis and the levels of IDO, respectively.

MenSCs were treated with 100 ng/mL IFN-γ (low concentration) or 200 ng/mL IFN-γ (high concentration) to determine the appropriate concentration for treatment. To accurately mimic the environment in which MenSCs perform their biological functions, we exposed MenSCs to H/R 72 h after priming[14,18]. Then, the cells were stained with Annexin V and propidium iodide (PI), and the proportions of apoptotic MenSCs in the different treatment groups were analyzed by flow cytometry. We found that H/R slightly increased stem cell apoptosis, but the difference was not significant (Figures 2E and F). Moreover, MenSCs that were primed with low and high IFN-γ concentrations were less resistant to H/R-induced apoptosis, and the overall proportions of apoptotic cells reached approximately 10% and 17%, respectively (Figures 2E and F). To maintain a relatively good state of MenSCs after intervention, we used the lower concentration of 100 ng/mL to prim MenSCs in the subsequent experiments.

As previously mentioned, IDO secreted by MSCs plays a key role in the regulation of T cells, and this metabolite can induce the differentiation of Tregs and thus promote immune tolerance[15,16]. Therefore, we used the IDO levels as an indicator to evaluate the efficacy of priming. The mRNA and protein levels of IDO in MenSCs were measured by qRT-PCR and western blotting, respectively, and the concentrations of IDO that were secreted by MenSCs were measured by ELISA. These results showed that the expression of IDO in MenSCs was upregulated 24 h after IFN-γ priming and reached a high level at 72 h. In addition, IDO continued to be expressed at a high level in MenSCs under H/R treatment conditions after the removal of IFN-γ (Figures 2G and H). Measurement of the IDO levels by ELISA showed that IDO was gradually secreted into the cell culture medium after priming, and when IFN-γ was removed after 72 h of priming, a considerable amount of IDO continued to be secreted by MenSCs under H/R treatment conditions (Figure 2I).

These results indicated that MenSCs could be maintained in a relatively good cell state when exposed to H/R after treatment with a low concentration of IFN-γ. Additionally, IFN-γ priming for 72 h promoted the expression and continuous secretion of IDO by MenSCs. Therefore, we chose 100 ng/mL IFN-γ for 72 h as the strategy for priming MenSCs to ensure that priming would be safe and effective.

IFN-γ-primed MenSCs attenuated liver IRI in the mouse short-term I/R model

The grouping and timeline of the animal experiments are shown in Figure 1. We administered MenSCs and IFN-γ-primed MenSCs (primed MenSCs) to short-term I/R model mice to explore their therapeutic potential. We found that the mice in the IR group showed significant hepatocyte injury after 6 h of reperfusion; this injury manifested as vacuole formation, increased inflammatory cell infiltration, disordered hepatic lobules, and tissue necrosis (Figure 3A), and these effects were accompanied by elevated serum levels of AST and ALT, which are indicators of liver function (Figures 3E and F), and relatively high Suzuki's injury scores (Figure 3B). However, the administration of MenSCs and primed MenSCs resulted in decreased ALT and AST levels, ameliorated IRI, and decreased Suzuki's injury scores (Figures 3A, B, E and F). Additionally, caspase-3 and TUNEL staining of liver tissue sections were performed to observe apoptosis. We reached the same conclusion, namely, that both MenSCs and IFN-primed MenSCs could attenuate I/R-induced hepatocyte apoptosis (Figures 3C and D). Moreover, these results also showed that primed MenSCs exerted a better therapeutic effect than
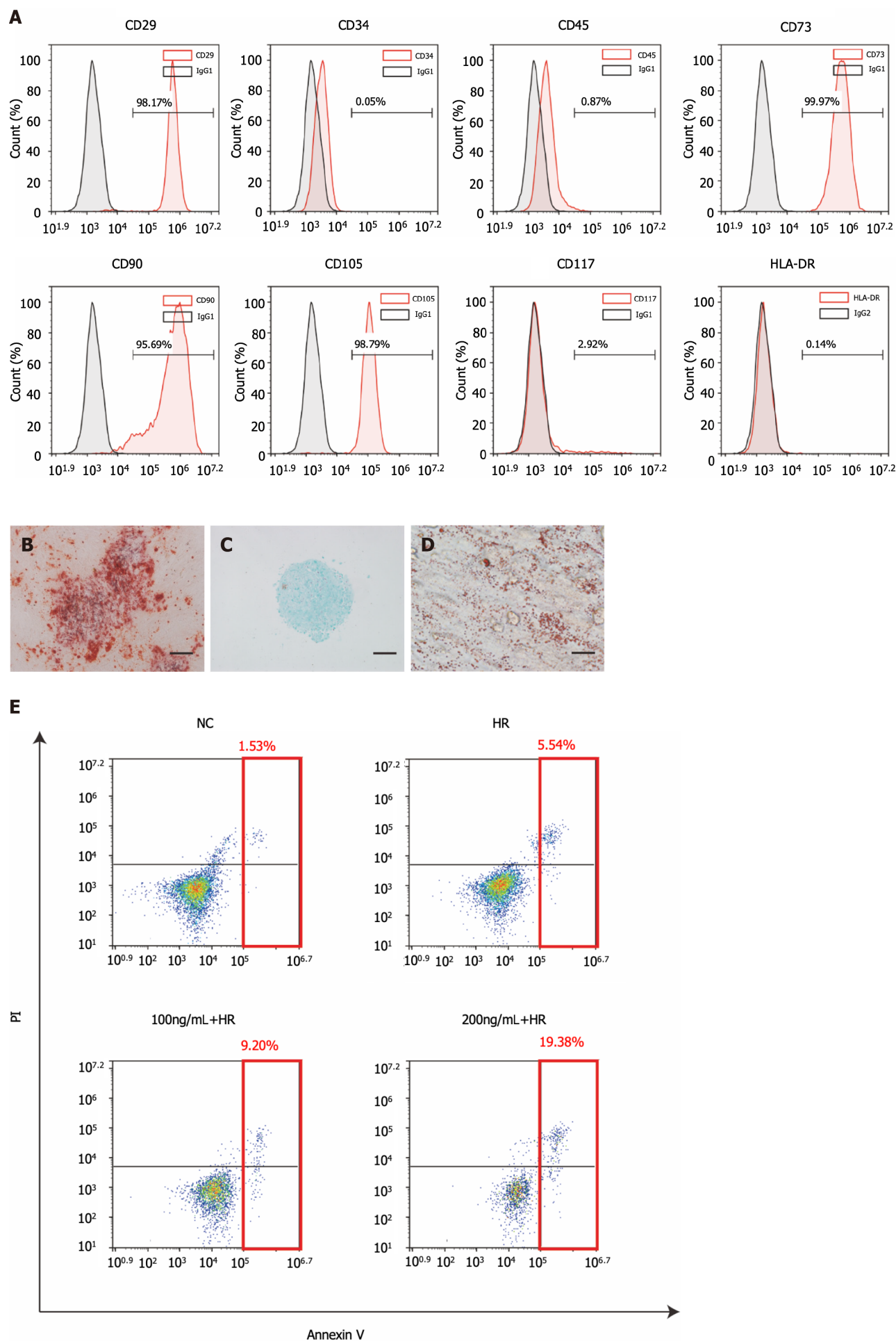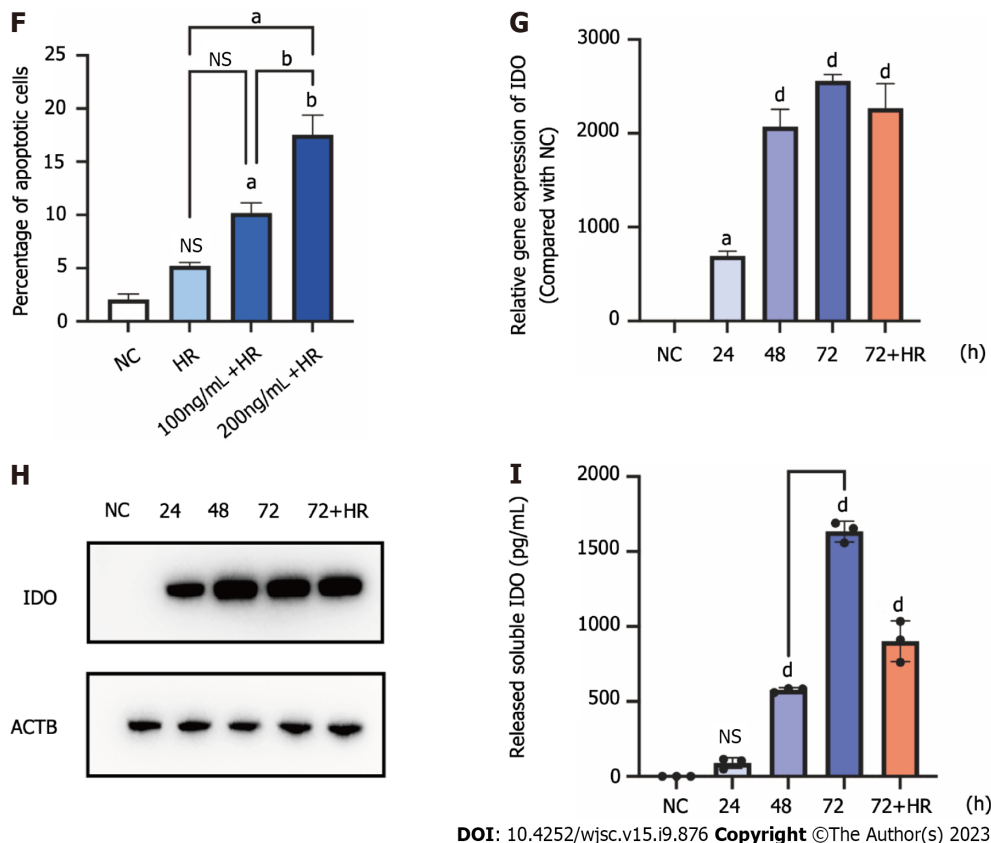
Figure 2 Characterization of menstrual blood-derived stromal cells and menstrual blood-derived stromal cells primed with interferon-γ. A: The surface marker expression of menstrual blood-derived stromal cells (MenSCs) was assessed by flow cytometry analysis; B: The osteogenic differentiation potential of MenSCs. Scale bar 200 µm; C: The chondrogenic differentiation potential of MenSCs. Scale bar 200 µm; D: The adipogenic differentiation potential of MenSCs. Scale bar 200 µm; E: MenSC apoptosis was detected by flow cytometry. The red box indicates the sum of late and early apoptotic cells, which represent the overall level of apoptosis; F: The overall level of apoptosis was analyzed; G: After MenSC priming with 100 ng/mL interferon-γ for 24 h, 48 h, 72 h, and 72 h + hypoxia/reoxygenation, the mRNA levels of indoleamine 2,3-dioxygenase (IDO) in MenSCs were determined by quantitative real-time reverse transcription polymerase chain reaction analysis; H: The protein level of IDO in MenSCs was determined by western blotting; I: The level of IDO secreted by MenSCs into the cell culture supernatant was measured by ELISA. The data are shown as the means ± SEMs, n = 3. [a]P < 0.05, [b]P < 0.01, [c]P < 0.001, [d]P < 0.0001. NS represents not statistically significant. All P values were obtained by one-way ANOVA. HLA-DR: Human leukocyte antigen-DR; IgG: Immunoglobulin G; NC: Negative control; HR: Hypoxia/reoxygenation; PI: Propidium iodide; IDO: Indoleamine 2,3-dioxygenase.

untreated MenSCs (Figures 3A-F).

IFN-γ-primed MenSCs reduced hepatocellular damage and increased the Treg numbers in the mouse long-term I/R model

As IFN-γ-primed MenSCs could exert a better therapeutic effect in the short-term model, we used 7 d of reperfusion after I/R to establish a long-term model in order to further explore the long-term effects of primed MenSCs, particularly their potential to induce immune tolerance.

We found that after 7 d of ischemia, the liver tissues of the mice showed obvious edema, a large cavity, and necrosis, and these conditions resulted in high Suzuki's injury scores. However, MenSCs and particularly IFN-γ-primed MenSCs significantly inhibited these changes (Figures 4A and B). Additionally, we determined the Treg numbers in the spleen to assess the immune tolerance of the mice. To determine the number of Tregs, we analyzed the percentage of cells that were positive for CD4, CD25, and Foxp3. Tregs accounted for approximately 1% of the total lymphocyte population in the sham and IR groups, and primed MenSCs increased the percentage of Tregs in the lymphocyte population to a great extent (Figures 4C and D). However, although untreated MenSCs also increased the percentage of Tregs, no significant difference was found compared with the sham group (Figures 4C and D). To verify the correlation between the stronger immunomodulatory ability of primed MenSCs and IDO, we added 1MT to the drinking water of some mice and found that 1MT clearly reversed the increase in the percentage of Tregs in the spleen and inhibited the protective effect of primed MenSCs on the liver (Figures 4A-D).

These results indicated that after 7 d of reperfusion, IFN-γ-primed MenSCs exerted a stronger and more stable effect on reducing liver injury and increasing the percentage of Tregs in the spleen compared with untreated MenSCs. These stronger therapeutic effects were closely associated with IDO.
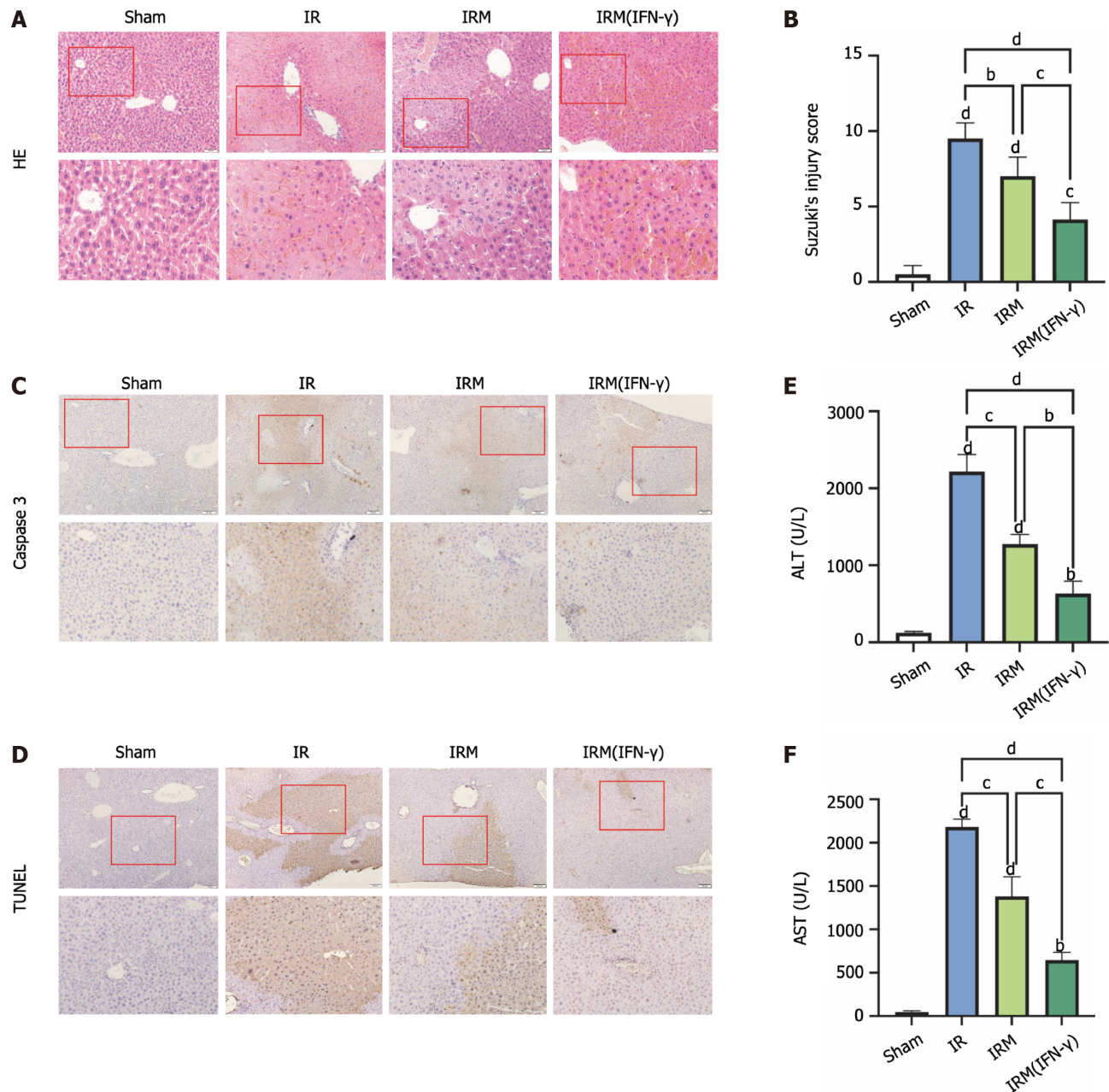
Figure 3 Interferon-γ-primed menstrual blood-derived stromal cells attenuated liver ischemia-reperfusion injury in the mouse short-term ischemia-reperfusion model. A: Representative images of histological liver sections stained with hematoxylin and eosin (hematoxylin and eosin staining, magnification 200 ×, images in the second row are partial magnifications of regions indicated by the red box); B: The degree of liver injury in each group was determined according to Suzuki's injury score. The data are expressed as the means ± SEMs (*n* = 10/group); C: Representative images of liver sections from each group stained for caspase-3 to evaluate the apoptosis level (magnification 200 ×, images in the second row are partial magnifications of regions indicated by the red box); D: Representative liver sections from each group stained with TUNEL were obtained to evaluate the apoptosis level (magnification 200 ×, images in the second row are partial magnifications of regions indicated by the red box); E: The serum alanine aminotransferase levels were measured to indicate liver function levels, the data are expressed as the means ± SEMs (*n* = 3/group); F: The serum aspartate aminotransferase levels were measured to indicate liver function levels, and the data are expressed as the means ± SEMs (*n* = 3/group). [a]$P < 0.05$, [b]$P < 0.01$, [c]$P < 0.001$, [d]$P < 0.0001$. NS represents not statistically significant. All *P* values were obtained by one-way ANOVA. MenSCs: Menstrual blood-derived stromal cells; IFN-γ: Interferon-γ; IR: Ischemia-reperfusion; IRM: Combination treated with ischemia-reperfusion and menstrual blood-derived stromal cells; IRM (IFN-γ): Combination treated with ischemia-reperfusion and interferon-γ-primed menstrual blood-derived stromal cells; HE: Hematoxylin and eosin; TUNEL: Terminal deoxynucleotidyl transferase-mediated dUTP-biotin Nick End Labeling; ALT: Alanine aminotransferase; AST: Aspartate aminotransferase.

IFN-γ-primed MenSCs promoted autophagy in mouse livers

As described above, we verified that the more significant immunomodulatory effect of primed MenSCs was indeed related to IDO. Strikingly, the more significant effect of primed MenSCs in alleviating liver injury was also associated with IDO. To explore the specific mechanism through which primed MenSCs ameliorate IRI, metabolomics sequencing of mouse liver samples from the short-term model was performed.
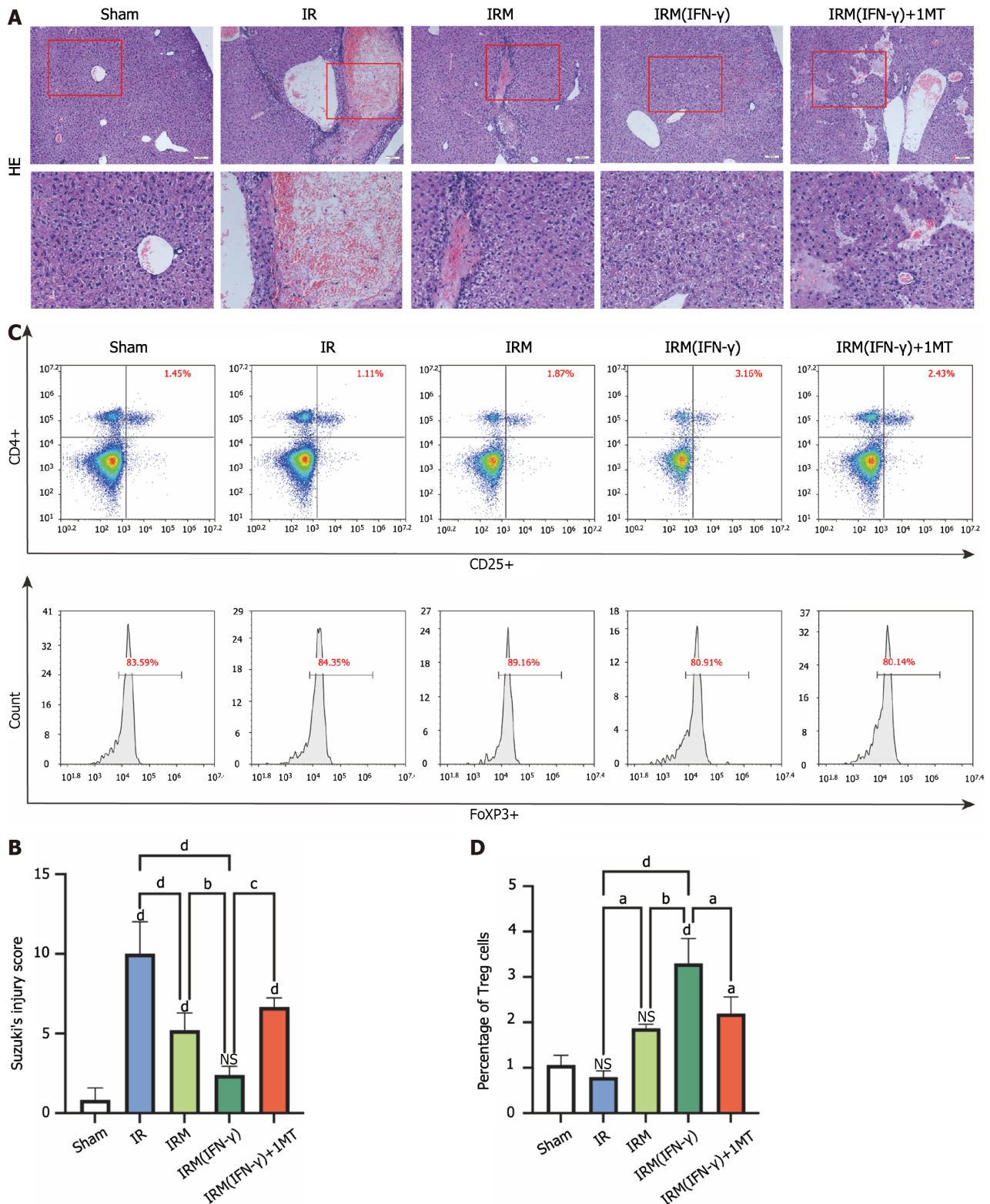
Figure 4 Interferon-γ-primed menstrual blood-derived stromal cells reduced hepatocellular damage and increased the Treg numbers in the mouse long-term ischemia-reperfusion model. A: Representative images of histological liver sections stained with hematoxylin and eosin were obtained (hematoxylin and eosin staining, magnification 200×, images in the second row are partial magnifications of regions indicated by the red box); B: The degree of liver injury in each group was determined according to Suzuki's injury score. The data are expressed as the means ± SEMs (n = 3-5/group); C: The numbers of CD4, CD25, and FoXP3 positive cells (regulatory T cells) in the spleen were determined by flow cytometry to estimate the ability of primed menstrual blood-derived stromal cells to induce immune tolerance; D: The percentages of Tregs are expressed as the means ± SEMs (n = 3/group). [a]$P < 0.05$, [b]$P < 0.01$, [c]$P < 0.001$, [d]$P < 0.0001$. NS represents not statistically significant. All P values were obtained by one-way ANOVA. MenSCs: Menstrual blood-derived stromal cells; IFN-γ: Interferon-γ; 1MT: 1-methyl-D-tryptophan; IR: Ischemia-reperfusion; IRM: Combination treated with ischemia-reperfusion and menstrual blood-derived stromal cells; IRM (IFN-γ): Combination treated with ischemia-reperfusion and interferon-γ-primed menstrual blood-derived stromal cells; HE: Hematoxylin and eosin; Treg: Regulatory T cell.

PCA and PLS-DA of samples from the two groups were performed to evaluate the degree of aggregation and dispersion of samples within a single group as well as between different groups, and the results indicated that the data could be used for subsequent analysis (Supplementary Figures 1A-D). A statistical heatmap of 45 metabolites that differed between the IR group and IRPM group [IRM (IFN-γ) group] was generated, and the results are also shown in the form of a volcano plot (Figures 5A and B). Kyoto Encyclopedia of Genes and Genomes (KEGG) annotation of the differential metabolites revealed that the differential metabolites are involved in a variety of biological processes, mainly including lipid metabolism, amino acid metabolism, signaling molecule transduction, and membrane transport (Figure 5C). To further elucidate the main biological functions of the differential metabolites, we performed KEGG pathway enrichment analysis of these differential metabolites, and the results showed that the differential metabolites were mainly enriched in autophagy (Figure 5D). Relative quantification of the level of the differential metabolite phosphatidyl ethanolamine (PE), which is related to autophagy, showed that treatment with IFN-γ-primed MenSCs increased the levels of PE in the livers (Figure 5E). The main role of PE in autophagy is mediating the formation of the autophagy membrane marker LC3II from LC3I. A higher PE level is related to a higher level of autophagy[22-25]. Therefore, we hypothesized that primed MenSCs may increase the level of autophagy in mouse liver tissues.

To further verify this hypothesis, we observed the autophagic bodies in mouse liver cells by transmission electron microscopy (TEM) and measured the expression of autophagy-related proteins in liver tissues by western blotting to evaluate the autophagy levels. MenSCs, and primed MenSCs increased the number of autophagosomes in liver tissues, and the increase was most obvious in the IRM (IFN-γ) group (Figures 6A and B). Consistent with the TEM results, LC3II expression was increased after I/R, suggesting that I/R could increase the level of autophagy in hepatocytes (Figures 6C and D). Moreover, the autophagic flux was amplified by MenSCs and particularly by primed MenSCs (Figures 6C and D). Additionally, we observed the changes in the AMPK pathway and the mTOR pathway, which are two classical pathways that are upstream of autophagy, and we found that I/R could promote AMPK phosphorylation and inhibit mTOR phosphorylation; in other words, I/R could activate the AMPK pathway and inhibit the mTOR pathway (Figures 6C and D). Moreover, most of these effects were enhanced by MenSCs and particularly primed MenSCs (Figures 6C and D).

In conclusion, we demonstrated that primed MenSCs amplified I/R-induced autophagy in the mouse livers through metabolome sequencing analysis and molecular biology experiments. However, the relationship between the enhanced autophagy and IDO and whether autophagy is related to the therapeutic effect of MenSCs in alleviating IRI still need to be further clarified.

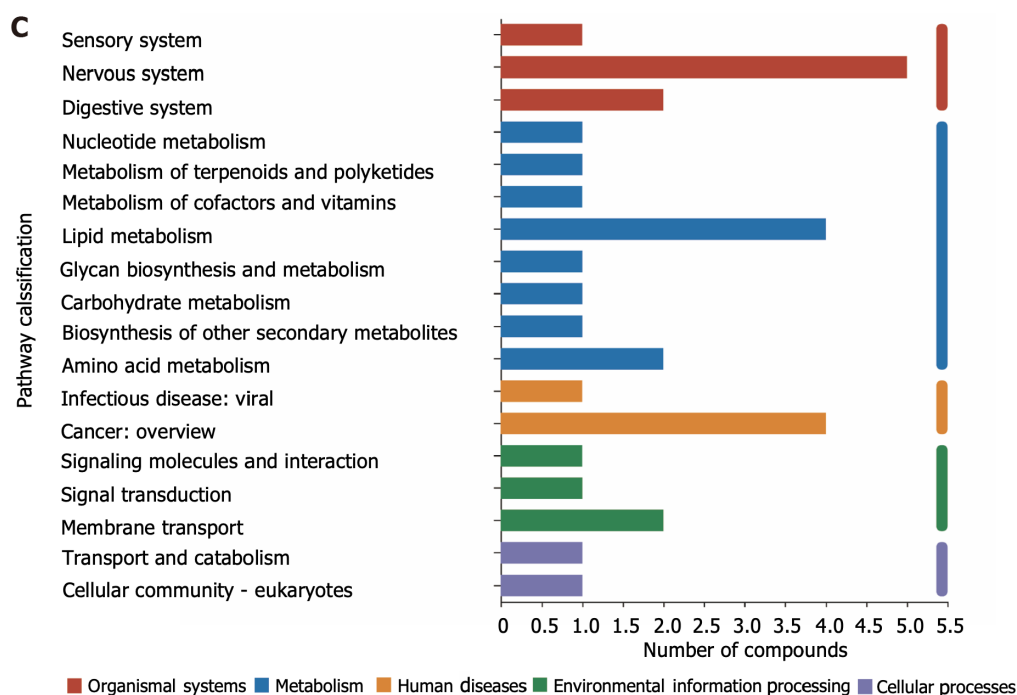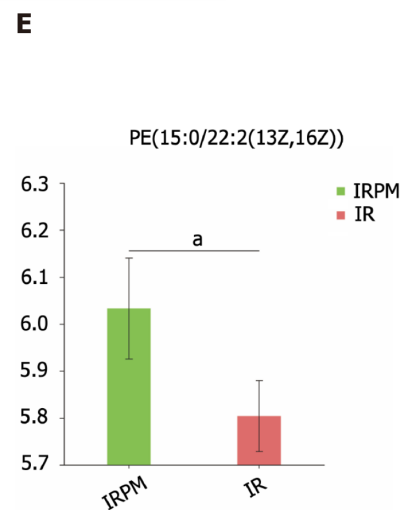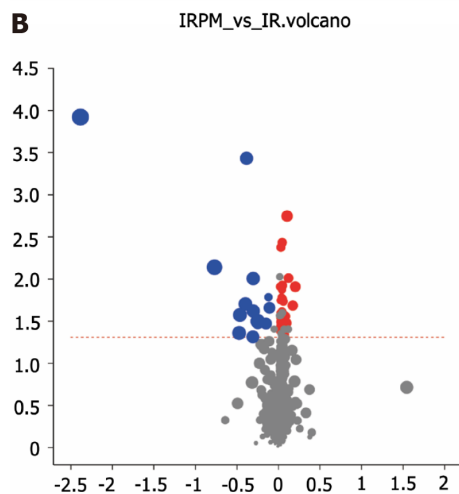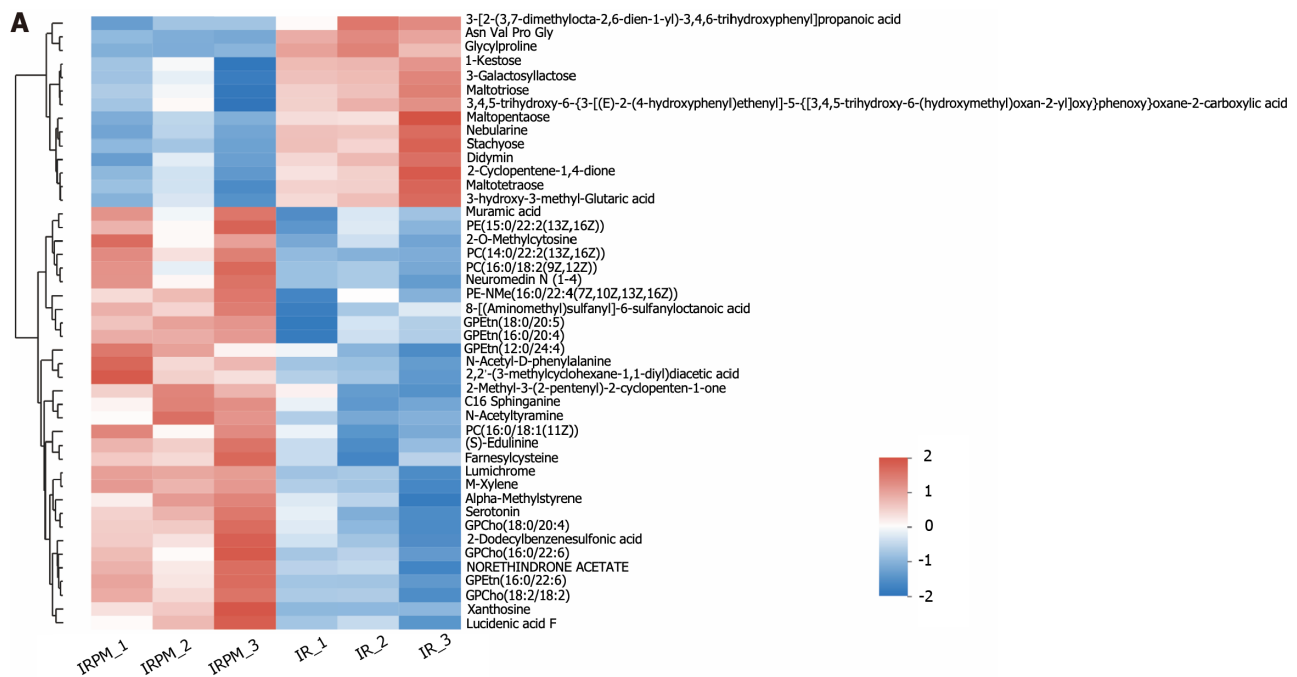### IFN-γ-primed MenSCs decreased H/R-induced hepatocyte apoptosis via autophagy and IDO

To further investigate the relationship among the therapeutic effect of primed MenSCs, IDO, and enhanced autophagy, we established an *in vitro* H/R model in L02 cells with the corresponding treatment conditions.

First, we exposed L02 cells to H/R for different times to determine an approximately appropriate H/R time. Autophagy-related protein levels were measured by western blotting. The AMPK pathway activation that was caused by hypoxia gradually decreased with increases in the reoxygenation time, and primed MenSCs delayed this process (Supplementary Figure 2A). In addition, we observed that autophagy-related protein expression changed in a time-dependent manner in the mouse model (Supplementary Figure 2B). To allow significant comparisons, we selected 6 h of hypoxia and 4 h of reoxygenation as the H/R conditions.

Apoptotic cells were identified by PI/Annexin V staining, and flow cytometry was performed to analyze cells that were exposed to different treatments. Cells in the upper right corner represent late apoptotic cells, cells in the lower right corner represent early apoptotic cells, and the sum of these two populations represents the overall level of apoptosis. We treated LO2 cells with 3MA (an autophagy inhibitor), 1MT (an IDO inhibitor), MenSCs, and primed MenSCs under normoxic conditions. These treatments alone did not significantly affect apoptosis under normoxic conditions (Figures 7A and B). After H/R, significant L02 cell apoptosis was observed, and the total apoptotic cell proportion accounted for approximately 14.89% of the overall cell population. After treatment of the cells with 3MA to inhibit autophagy under H/R conditions, the total apoptotic cell proportion accounted for approximately 45.06% of the overall cell population (Figures 7A and B). This finding indicated that H/R induced L02 cell apoptosis, and inhibition of autophagy significantly increased H/R-induced apoptosis. In addition, we also observed that the proportion of apoptotic cells was significantly reduced after coculture with MenSCs and particularly with primed MenSCs under H/R conditions, and this result indicated that stem cells can protect L02 cells from H/R-induced apoptosis (Figures 7A and B). A comparison of the HRM (IFN-γ) and HRM (IFN-γ) + 3MA groups revealed that the protective effect of primed MenSCs was significantly reduced when autophagy was inhibited (Figures 7A and B). This finding indicated that primed MenSCs may protect L02 cells against H/R by enhancing autophagy. In addition, a comparison of the HRM (IFN-γ) and HRM (IFN-γ) + 1MT groups showed that inhibition of IDO by 1MT also inhibited the protective effect of primed MenSCs (Figures 7A and B). These results indicated that autophagy reduced H/R-induced apoptosis and that the more powerful protective effect of IFN-γ-primed MenSCs was closely associated with autophagy and IDO.

IDO secreted by primed MenSCs enhanced autophagy by inhibiting the mTOR pathway and activating the AMPK pathway

As mentioned above, primed MenSCs attenuated H/R-induced apoptosis *via* IDO and autophagy. To further investigate whether IDO is related to autophagy, we used 1MT to inhibit IDO and observed changes in autophagy. L02 cells were transfected with pCMV-GFP-LC3, exposed to the indicated treatments and then observed under a fluorescence microscope. We counted the number of intense punctate GFP-LC3 aggregates in each cell to assess autophagy. The results showed that H/R increased the level and aggregation of GFP-LC3 in cells, and this phenomenon was amplified by MenSCs and particularly by primed MenSCs (Figures 8A and B). In addition, the effect of primed MenSCs on GFP-LC3
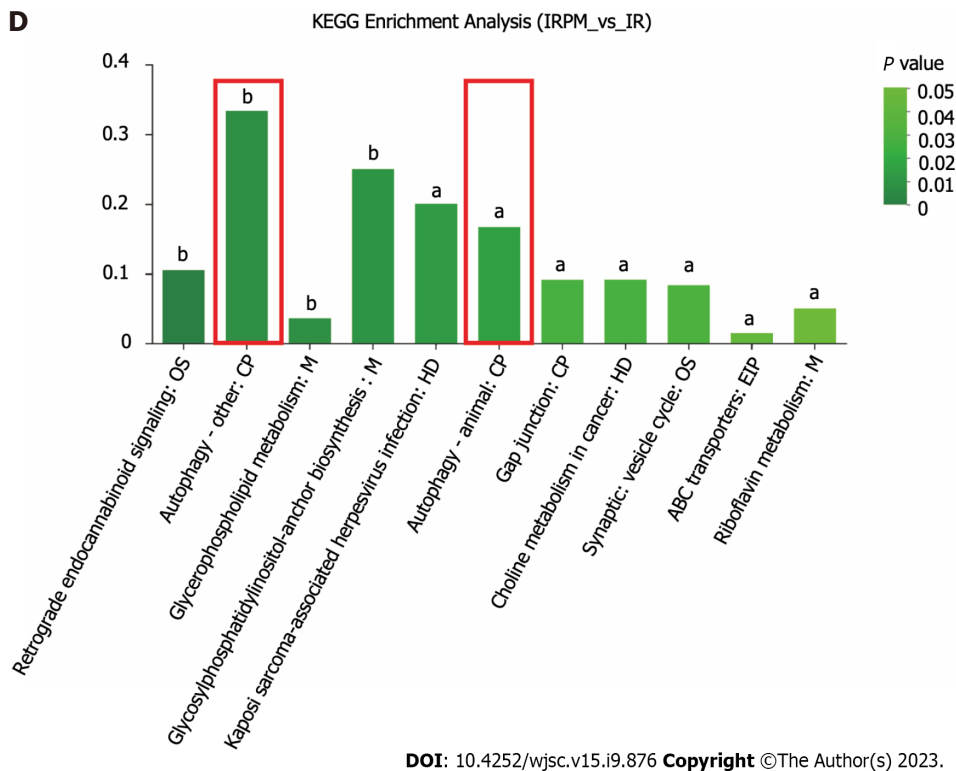
A

3-[2-(3,7-dimethylocta-2,6-dien-1-yl)-3,4,6-trihydroxyphenyl]propanoic acid
Asn Val Pro Gly
Glycylproline
1-Kestose
3-Galactosyllactose
Maltotriose
3,4,5-trihydroxy-6-{3-[(E)-2-(4-hydroxyphenyl)ethenyl]-5-{[3,4,5-trihydroxy-6-(hydroxymethyl)oxan-2-yl]oxy}phenoxy}oxane-2-carboxylic acid
Maltopentaose
Nebularine
Stachyose
Didymin
2-Cyclopentene-1,4-dione
Maltotetraose
3-hydroxy-3-methyl-Glutaric acid
Muramic acid
PE(15:0/22:2(13Z,16Z))
2-O-Methylcytosine
PC(14:0/22:2(13Z,16Z))
PC(16:0/18:2(9Z,12Z))
Neuromedin N (1-4)
PE-NMe(16:0/22:4(7Z,10Z,13Z,16Z))
8-[(Aminomethyl)sulfanyl]-6-sulfanyloctanoic acid
GPEtn(18:0/20:5)
GPEtn(16:0/20:4)
GPEtn(12:0/24:4)
N-Acetyl-D-phenylalanine
2,2'-(3-methylcyclohexane-1,1-diyl)diacetic acid
2-Methyl-3-(2-pentenyl)-2-cyclopenten-1-one
C16 Sphinganine
N-Acetyltyramine
PC(16:0/18:1(11Z))
(S)-Edulinine
Farnesylcysteine
Lumichrome
M-Xylene
Alpha-Methylstyrene
Serotonin
GPCho(18:0/20:4)
2-Dodecylbenzenesulfonic acid
GPCho(16:0/22:6)
NORETHINDRONE ACETATE
GPEtn(16:0/22:6)
GPCho(18:2/18:2)
Xanthosine
Lucidenic acid F

B

IRPM_vs_IR.volcano

- Up (red)
- Nosig (grey)
- Down (blue)

C

Pathway calssification:
- Sensory system
- Nervous system
- Digestive system
- Nucleotide metabolism
- Metabolism of terpenoids and polyketides
- Metabolism of cofactors and vitamins
- Lipid metabolism
- Glycan biosynthesis and metabolism
- Carbohydrate metabolism
- Biosynthesis of other secondary metabolites
- Amino acid metabolism
- Infectious disease: viral
- Cancer: overview
- Signaling molecules and interaction
- Signal transduction
- Membrane transport
- Transport and catabolism
- Cellular community - eukaryotes

Number of compounds

■ Organismal systems ■ Metabolism ■ Human diseases ■ Environmental information processing ■ Cellular processes

E

PE(15:0/22:2(13Z,16Z))

■ IRPM ■ IR

a

D

Figure 5 Metabolomic data analysis. A: Heatmap of 45 differential metabolites between the ischemia-reperfusion (IR) group and IRM (interferon-γ) group; B: Volcano plot of 45 differential metabolites; C: The relevant pathways in which the differential metabolites are involved were analyzed by comparing the information in the Kyoto Encyclopedia of Genes and Genomes database; D: The main biological functions of differential metabolites were elucidated by pathway enrichment analysis; E: Relative quantitation of the differential metabolite phosphatidyl ethanolamine was performed to measure the effect of primed menstrual blood-derived stromal cells on the level of autophagy in liver tissues. MenSCs: Menstrual blood-derived stromal cells; IFN-γ: Interferon-γ; IR: Ischemia-reperfusion; IRM(IFN-γ) or IRPM: Combination treated with ischemia-reperfusion and interferon-γ-primed menstrual blood-derived stromal cells; PE: Phosphatidyl ethanolamine; OS: Organismal systems; M: Metabolism; HD: Human diseases; CP: Cellular processes; EIP: Environmental information processing; KEEG: Kyoto Encyclopedia of Genes and Genomes.

punctate aggregation was reversed by 1MT, which suggested that IDO was related to the promotion of autophagy (Figures 8A and B). Then, we measured the changes in autophagy-related protein expression by western blotting to further explore how IDO affects autophagy. The results showed that H/R could inhibit the mTOR pathway, activate the AMPK pathway, and increase autophagy, and these effects were enhanced by MenSCs and particularly by primed MenSCs (Figures 8C and D); furthermore, the enhanced effect of primed MenSCs on autophagy was reversed by the IDO inhibitor 1MT (Figures 8C and D). These results indicated that IDO secreted by primed MenSCs enhanced autophagy by inhibiting the mTOR pathway and activating the AMPK pathway.

DISCUSSION

In this study, we found that IDO secreted by IFN-γ-primed MenSCs enhanced the therapeutic effect of MenSCs in the mouse liver I/R model, and the related mechanisms are shown in Figure 9. However, some studies have indicated that the combination of IFN-γ and tumor necrosis factor-alpha (TNF-α) could more efficiently promote the secretion of IDO by MSCs[12]. Although our study showed that priming with 100 ng/mL IFN-γ for 72 h was sufficient to initiate IDO secretion by MenSCs, priming with multiple inflammatory factors to generate better and more functional MenSCs still has a very high experimental value. However, considering that the high concentration of IFN-γ decreased the tolerance of MenSCs to H/R-induced injury (Figures 2E and F), we hypothesized that the priming of MenSCs with multiple inflammatory cytokines may cause more severe damage. Consequently, the side effects of these inflammatory cytokines on MSCs need to be further investigated *in vitro* and *in vivo*.

In addition to priming MSCs with some inflammatory factors, such as transforming growth factor-β, IL-17, TNF-α, and IFN-γ, to promote the secretion of immune regulatory cytokines[26-28], MSCs could also be modified by gene editing to overexpress some immune regulatory factors and thus enhance their therapeutic effects. In one study, MSCs that overexpressed IDO were more effective in alleviating injury in dilated cardiomyopathy in mice and further enhanced the responses of Tregs and Th2 cells[29]. Therefore, subsequent studies may examine the differences in safety, efficacy, and cost between these two approaches to identify the more suitable method of MSC modification.
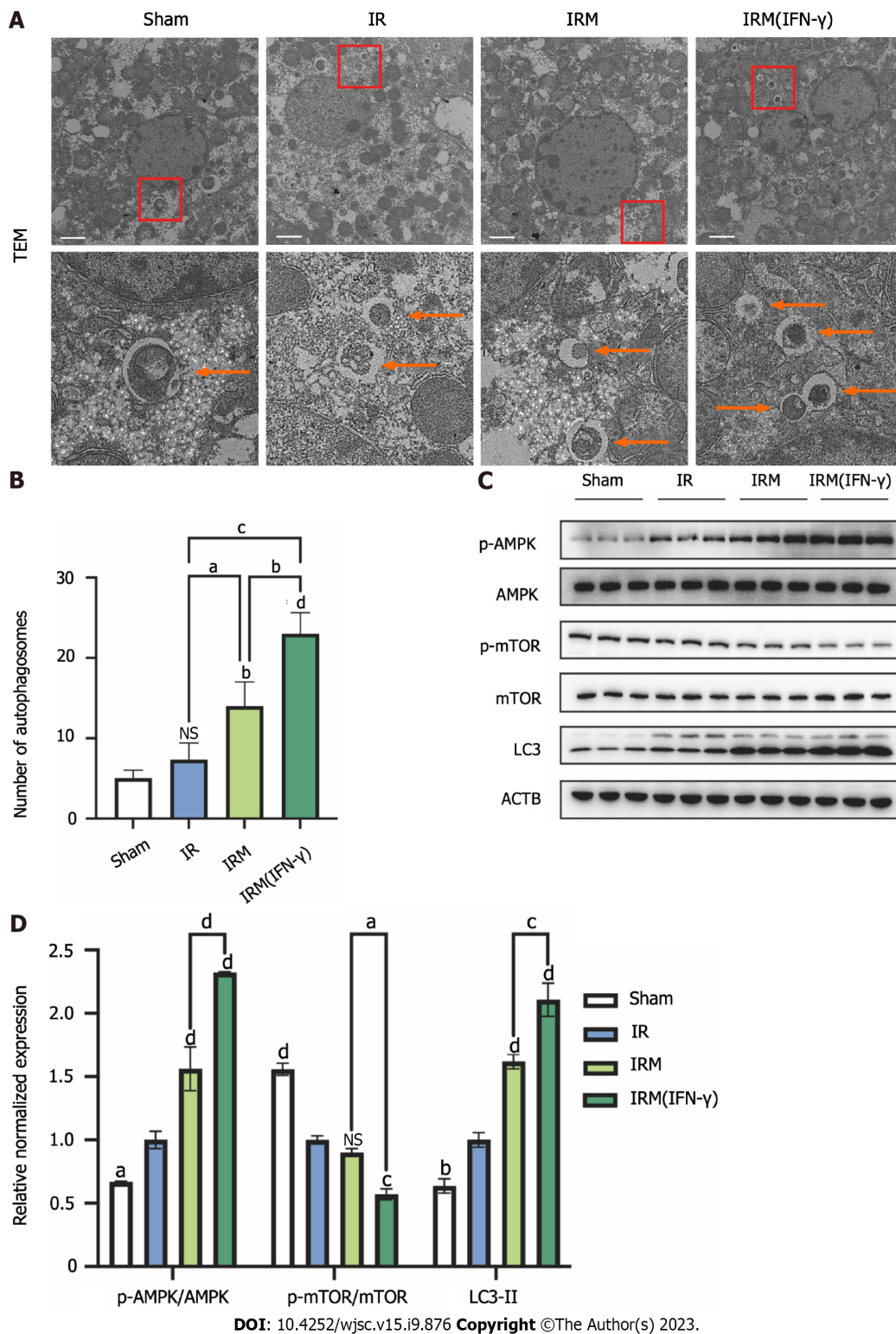
Figure 6 Interferon-γ-primed menstrual blood-derived stromal cells enhanced autophagy in mouse livers. A: Representative TEM images were used to determine the number of autophagic vacuoles in liver tissues from each experimental group. Scale bar 2 μm. The images in the second row are partial magnifications of the regions indicated by the red box; B: The number of autophagosomes was counted by TEM. The data are expressed as the means ± SEMs (n = 3/group); C: The expression of p-AMPK, AMPK, p-mammalian target of rapamycin (p-mTOR), mTOR, LC3, and ACTB in liver tissues was determined by western blotting; D: The relative normalized expression was quantified based on the intensities of the western blot bands (n = 3/group). The data are presented as the means ± SEMs. [a]$P < 0.05$, [b]$P < 0.01$, [c]$P < 0.001$, [d]$P < 0.0001$. NS represents not statistically significant. All P values were obtained by one-way ANOVA. MenSCs: Menstrual blood-derived stromal cells; IFN-γ: Interferon-γ; IR: Ischemia-reperfusion; IRM: Combination treated with ischemia-reperfusion and menstrual blood-derived stromal cells; IRM (IFN-γ): Combination treated with ischemia-reperfusion and interferon-γ-primed menstrual blood-derived stromal cells; TEM: Transmission electron microscopy; AMPK: The AMP-activated protein kinase signaling pathway; mTOR: Mammalian target of rapamycin; Tregs: Regulatory T cells.
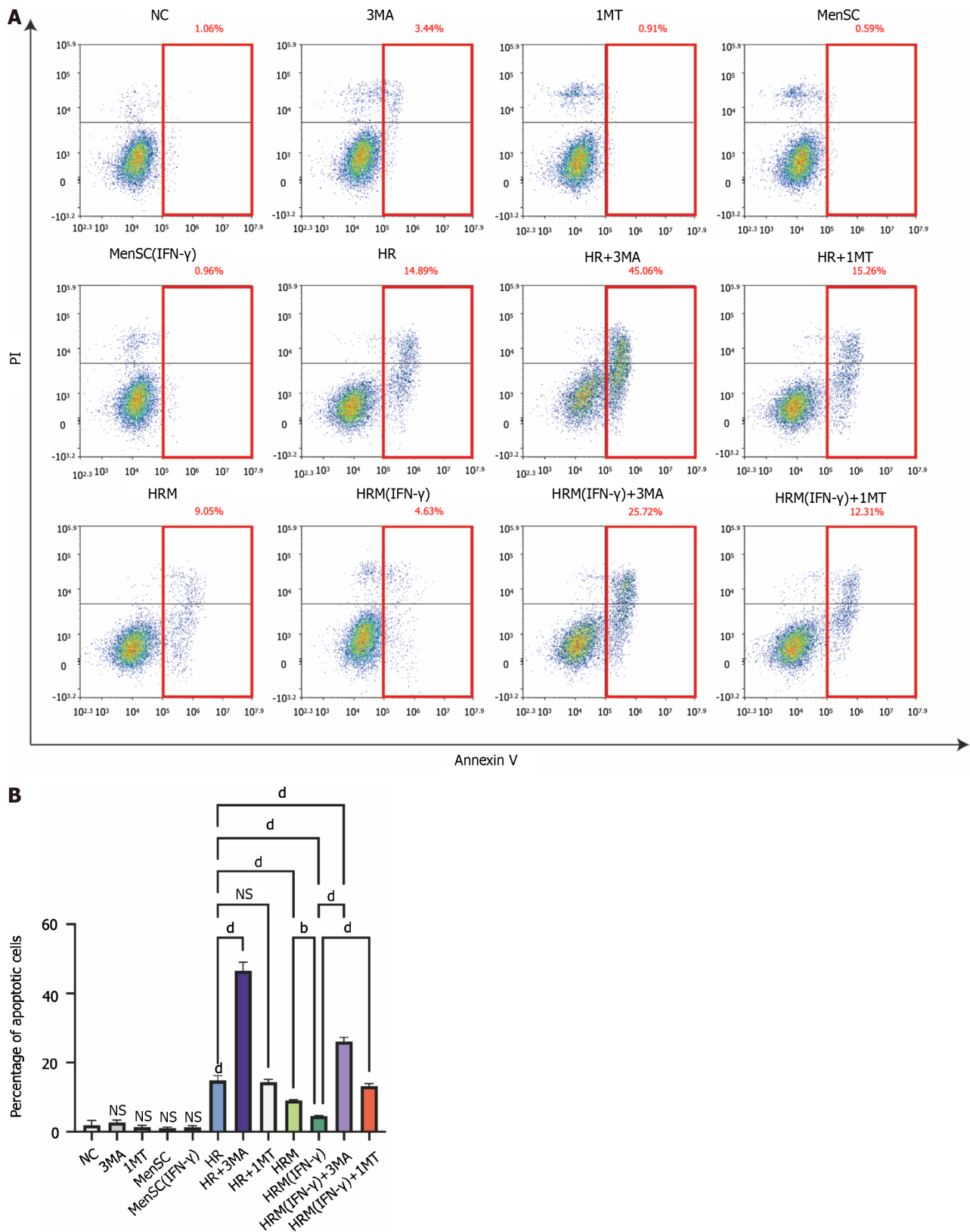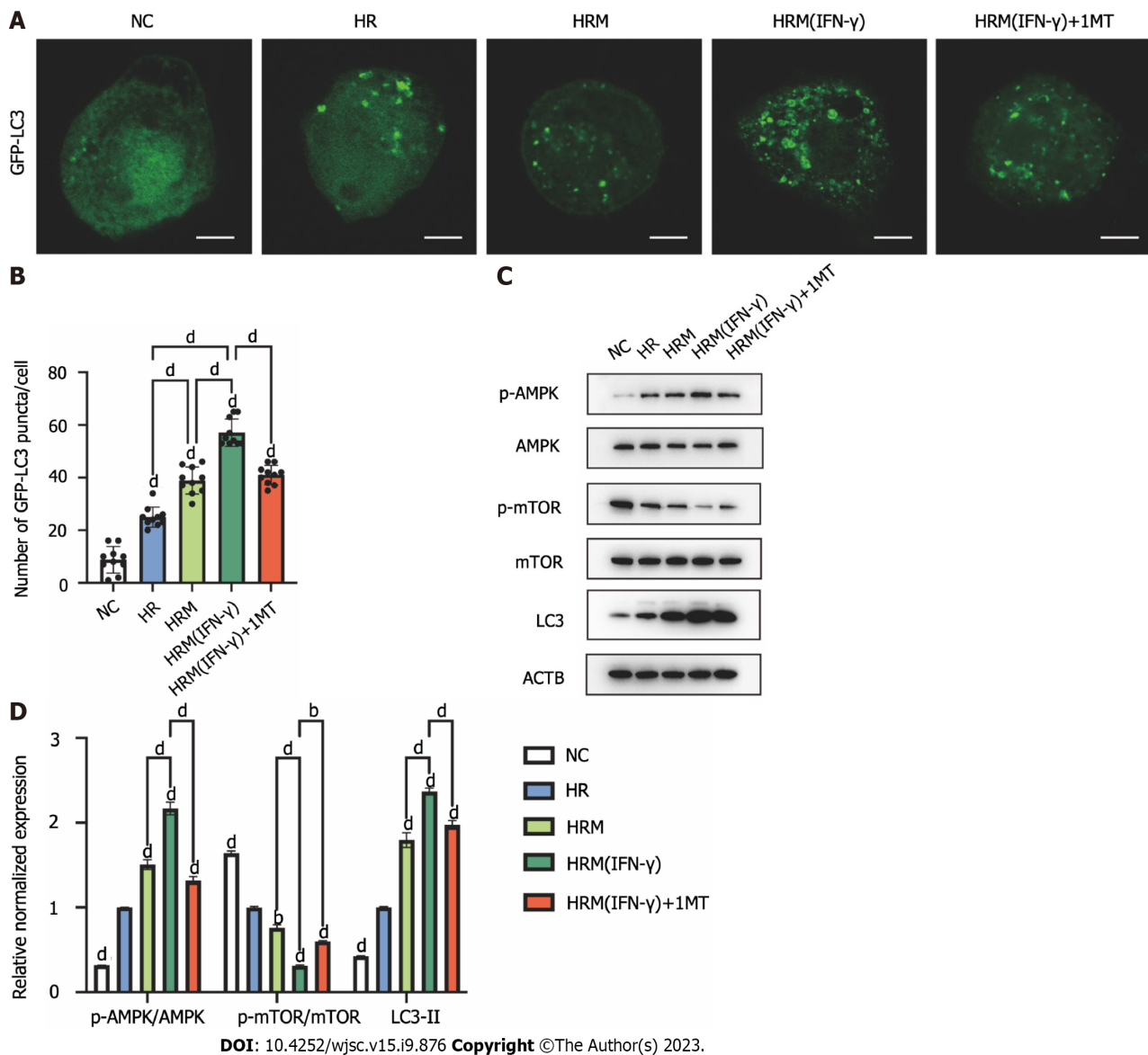
Figure 7 interferon-γ-primed menstrual blood-derived stromal cells decreased hypoxia/reoxygenation-induced cell apoptosis *via* autophagy and indoleamine 2,3-dioxygenase. A: Apoptosis of L02 cells after different treatments was analyzed; B: The sum of the percentage of early apoptotic cells and late apoptotic cells was analyzed. The total percentage of apoptotic cells (sum of the percentage of early apoptotic cells and late apoptotic cells) was analyzed. The data are shown as the mean ± SEM, n = 3; [b]P < 0.01, [d]P < 0.0001. NS represents not statistically significant. All P values were obtained by one-way ANOVA. PI: Propidium iodide; NC: Negative control; 3MA: 3-methyladenine; 1MT: 1-methyl-D-tryptophan; MenSCs: Menstrual blood-derived stromal cells; IFN-γ: Interferon-γ; HR: Hypoxia/reoxygenation; HRM: Combination treated with hypoxia/reoxygenation and menstrual blood-derived stromal cells; HRM (IFN-γ): Combination treated with hypoxia/reoxygenation and I interferon-γ-primed menstrual blood-derived stromal cells.

Figure 8 Indoleamine 2,3-dioxygenase secreted by interferon-γ-primed menstrual blood-derived stromal cells enhanced autophagy by inhibiting the mammalian target of rapamycin pathway and activating the AMPK pathway. A: Immunofluorescence images of GFP-LC3. Scale bar 2 μm; B: The number of intense punctate GFP-LC3 aggregates in each cell was counted to determine the level of autophagy in each group. The data are expressed as the means ± SEMs (*n* = 10/group); C: The expression of p-AMPK, AMPK, p-mammalian target of rapamycin (p-mTOR), mTOR, LC3, and ACTB in L02 cells was determined by western blotting; D: The relative normalized protein expression was quantified based on the intensities of the western blot bands (*n* = 3/group). The data are presented as the means ± SEMs. $^{a}P < 0.05$, $^{b}P < 0.01$, $^{c}P < 0.001$, $^{d}P < 0.0001$. NS represents not statistically significant. All *P* values were obtained by one-way ANOVA. NC: Negative control; 3MA: 3-methyladenine; 1MT: 1-methyl-D-tryptophan; MenSCs: Menstrual blood-derived stromal cells; IFN-γ: Interferon-γ; HR: Hypoxia/reoxygenation; HRM: Combination treated with hypoxia/reoxygenation and menstrual blood-derived stromal cells; HRM (IFN-γ): Combination treated with hypoxia/reoxygenation and l interferon-γ-primed menstrual blood-derived stromal cells; AMPK: AMP-activated protein kinase; mTOR: the Mammalian target of rapamycin signaling pathway.

To date, 79 clinical trials involving the use of MSCs to prevent or treat graft-*versus*-host disease (GVHD) have been conducted[30]. Most of the studies demonstrated the safety and efficacy of MSCs, but some studies showed that MSCs did not exert the desired protective effect; differences in the immunomodulatory effects of MSCs may be related to the origin and the dose of MSCs that were used. One study compared the therapeutic potential of MSCs from different origins in a mouse GVHD model and found that bone marrow-derived MSCs (BM-MSCs) induced a rapid proinflammatory response before exerting immunosuppressive effects and that BM-MSCs were less capable of inducing Treg differentiation than umbilical cord blood-derived MSCs (UC-MSCs)[31]. Therefore, differences in the origin of MSCs might be a reason why some MSCs did not exert the expected effects in some studies[7,8]. It has also been suggested that subsequent studies on MSCs may focus on the differences in the therapeutic potential of MSCs that are derived from different sources. Moreover, another study showed that a double dose of UC-MSCs exerted a better therapeutic effect than a single dose of UC-MSCs in a rat dilated cardiomyopathy model[29]. Consequently, in addition to improving MSCs, selecting the right MSC source and the right MSC dose is also crucial for research.
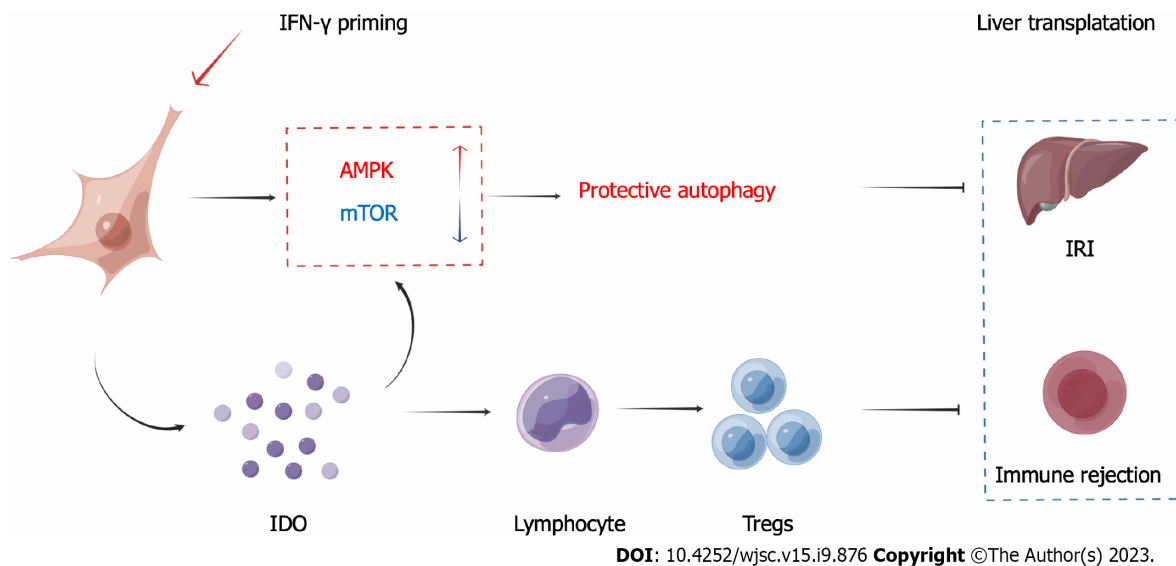
DOI: 10.4252/wjsc.v15.i9.876 **Copyright** ©The Author(s) 2023.

Figure 9 Schematic depiction of the mechanism. Ischemia-reperfusion injury (IRI) and immune rejection are two important factors that affect the prognosis of liver transplantation. After priming menstrual blood-derived stromal cells (MenSCs) with interferon-γ, the MenSCs secreted high levels of indoleamine 2,3-dioxygenase (IDO). On the one hand, MenSCs and IDO enhanced the AMPK-mammalian target of rapamycin-autophagy axis to reduce IRI; on the other hand, IDO promoted the differentiation of lymphocytes into Tregs to reduce immune rejection. IRI: Ischemia-reperfusion injury; MenSCs: Menstrual blood-derived stromal cells; IFN-γ: Interferon-γ; IDO: Indoleamine 2,3-dioxygenase; AMPK: AMP-activated protein kinase signaling pathway; mTOR: Mammalian target of rapamycin signaling pathway; Tregs: Regulatory T cells.

This study found that IDO secreted by IFN-γ-primed MenSCs was found to activate the AMPK pathway and inhibited the mTOR pathway, which resulted in inducing of protective autophagy in hepatocytes. However, the specific mechanism through which IDO activates the AMPK pathway or inhibits the mTOR pathway remains unclear. IDO is a metabolic enzyme that can promote tryptophan metabolism and produce kynurenine. Some studies have shown that IFN-γ priming and IDO overexpression can promote tryptophan depletion and kynurenine accumulation, and these phenomena induce autophagy in cervical cancer cells and promote phagocytosis by macrophages[32]. Studies have also shown that a protective autophagic response and amino acid metabolism, which are driven by IFN-γ-mediated induction of IDO enzyme activity, could inhibit antibody-mediated inflammatory kidney injury in a mouse model of nephrotoxic serum nephritis[33]. Another study showed that glucose metabolism is also related to the T cell inhibition caused by MSCs and IDO[34]. In this study, we found that primed MenSCs increased the relative expression of the autophagy-related metabolite PE in mouse livers, and corresponding experiments proved that primed MenSCs indeed promoted autophagy through IDO; however, we did not conduct targeted metabolomics analyses to quantify the absolute expression of PE. In addition, how IDO causes changes in the levels of PE are unclear. Therefore, further study is needed to determine how IDO triggers autophagy. Notably, tryptophan catabolism by IDO could alter inflammatory responses and favor T-cell tolerance in cancer[35,36]. Although there is no evidence showing that MSCs can promote tumor growth and our previous study showed that MSCs can inhibit the growth of hepatocellular carcinoma through epigenetic regulation[37], the use of primed MSCs in cancer patients may still be controversial.

In addition, because IDO secreted by MSCs could increase the Tregs to induce immune tolerance, as has been observed in several studies[14,17], we paid more attention to the potential of primed MenSCs to reduce liver IRI in this study, and only used the number of Tregs as an indicator to evaluate the MSC-induced - immune tolerance potential. Therefore, although primed MenSCs significantly increased the numbers of Tregs, it is still necessary to verify whether the increased Tregs could alleviate IRI[38] or better induce immune tolerance in the liver transplantation model. Besides, recent studies have shown that macrophage activation and neutrophil infiltration also play important roles in liver IRI[39,40], and the regulation of MSCs to different types of immune cells deserves further study.

Notably, untreated MenSCs could also activate the AMPK pathway, inhibit the mTOR pathway and enhance autophagy in the I/R or H/R models; however, untreated MenSCs secreted little IDO (Figures 2G-I). This finding indicates that the effect of MenSCs in enhancing autophagy is not entirely dependent on IDO and may be related to other mechanisms. How stem cells enhance autophagy in recipient cells is still worth further study.

CONCLUSION

IFN-γ-primed MenSCs could exert a better therapeutic effect in a liver I/R model than untreated MenSCs by secreting higher levels of IDO. On the one hand, MenSCs and IDO enhanced the AMPK-mTOR-autophagy axis to reduce IRI; on the other hand, IDO increased the Treg numbers in the spleen and enhanced the ability of MenSCs to induce immune tolerance. Our study suggests that IFN-γ-primed MenSCs may be a novel and improved MSC product for liver transplantation in the future.

ARTICLE HIGHLIGHTS

Research background

Ischemia-reperfusion injury (IRI) and immune rejection are two important factors that affect the prognosis of liver transplantation. Mesenchymal stem cells (MSCs) have been used in liver transplantation and showed certain beneficial effects.

Research motivation

Some studies have indicated that the effects of MSCs are not very significant. Therefore, there is an urgent to find a new way to make MSCs exert better therapeutic effect.

Research objectives

In this study, we attempted to enhance the therapeutic potential of human menstrual blood-derived stromal cells (MenSCs) in a mouse liver ischemia-reperfusion (I/R) model through interferon-γ (IFN-γ) priming strategies and explore the specific mechanisms.

Research methods

After determining the appropriate priming strategies, we applied MenSCs and primed MenSCs in the short-term and long-term mouse liver I/R models, and compared their therapeutic effects. In order to further explore the specific mechanism, we performed a metabolomic analysis of mouse liver samples.

Research results

IFN-γ-primed MenSCs secreted higher levels of indoleamine 2,3-dioxygenase (IDO), attenuated liver injury, and increased regulatory T cell (Treg) numbers in the mouse spleens to greater degrees than untreated MenSCs. Metabolomics and autophagy analyses proved that primed MenSCs more strongly induced protective autophagy in the mouse livers. Further experiments proved that IDO enhanced the protective autophagy by inhibiting the mammalian target of rapamycin (mTOR) pathway and activating the AMPK pathway.

Research conclusions

IFN-γ-primed MenSCs exerted better therapeutic effects in the liver I/R model through secreting higher IDO levels. IDO, on the one hand, increased Treg numbers in the spleen; on the other hand, activated the AMPK-mTOR-autophagy axis to reduce IRI.

Research perspectives

Our study suggests that IFN-γ-primed MenSCs may be a novel and superior MSC product for liver transplantation in the future, and the specific mechanism of how MSCs or IDO enhance autophagy in recipient cells is still worth further study.

Country/Territory of origin: China

ORCID number: Si-Ning Zhou 0000-0003-3680-2307; Li-Jun Chen 0000-0001-9374-6466; Hui-Kang Xu 0000-0001-8370-6444; Yi-Fei Li 0000-0003-3261-8182; Charlie Xiang 0000-0002-8194-2483.

S-Editor: Wang JJ
L-Editor: A
P-Editor: Zhang XD

REFERENCES

1 **Nakano R**, Tran LM, Geller DA, Macedo C, Metes DM, Thomson AW. Dendritic Cell-Mediated Regulation of Liver Ischemia-Reperfusion Injury and Liver Transplant Rejection. *Front Immunol* 2021; **12**: 705465 [PMID: 34262574 DOI: 10.3389/fimmu.2021.705465]

2 **Yang B**, Duan W, Wei L, Zhao Y, Han Z, Wang J, Wang M, Dai C, Zhang B, Chen D, Chen Z. Bone Marrow Mesenchymal Stem Cell-Derived Hepatocyte-Like Cell Exosomes Reduce Hepatic Ischemia/Reperfusion Injury by Enhancing Autophagy. *Stem Cells Dev* 2020; **29**: 372-379 [PMID: 31969065 DOI: 10.1089/scd.2019.0194]

3 **Yao J**, Zheng J, Cai J, Zeng K, Zhou C, Zhang J, Li S, Li H, Chen L, He L, Chen H, Fu H, Zhang Q, Chen G, Yang Y, Zhang Y. Extracellular vesicles derived from human umbilical cord mesenchymal stem cells alleviate rat hepatic ischemia-reperfusion injury by suppressing oxidative stress and neutrophil inflammatory response. *FASEB J* 2019; **33**: 1695-1710 [PMID: 30226809 DOI: 10.1096/fj.201800131RR]

4 **Grange C**, Bellucci L, Bussolati B, Ranghino A. Potential Applications of Extracellular Vesicles in Solid Organ Transplantation. *Cells* 2020; **9** [PMID: 32033489 DOI: 10.3390/cells9020369]

5 **Zheng J**, Chen L, Lu T, Zhang Y, Sui X, Li Y, Huang X, He L, Cai J, Zhou C, Liang J, Chen G, Yao J, Yang Y. MSCs ameliorate hepatocellular apoptosis mediated by PINK1-dependent mitophagy in liver ischemia/reperfusion injury through AMPKα activation. *Cell Death Dis* 2020; **11**: 256 [PMID: 32312955 DOI: 10.1038/s41419-020-2424-1]

6 **Shi M**, Liu Z, Wang Y, Xu R, Sun Y, Zhang M, Yu X, Wang H, Meng L, Su H, Jin L, Wang FS. A Pilot Study of Mesenchymal Stem Cell Therapy for Acute Liver Allograft Rejection. *Stem Cells Transl Med* 2017; **6**: 2053-2061 [PMID: 29178564 DOI: 10.1002/sctm.17-0134]

7 **Casiraghi F**, Perico N, Podestà MA, Todeschini M, Zambelli M, Colledan M, Camagni S, Fagiuoli S, Pinna AD, Cescon M, Bertuzzo V, Maroni L, Introna M, Capelli C, Golay JT, Buzzi M, Mister M, Ordonez PYR, Breno M, Mele C, Villa A, Remuzzi G; MSC-LIVER Study Group. Third-party bone marrow-derived mesenchymal stromal cell infusion before liver transplantation: A randomized controlled trial. *Am J Transplant* 2021; **21**: 2795-2809 [PMID: 33370477 DOI: 10.1111/ajt.16468]

8 **Vandermeulen M**, Erpicum P, Bletard N, Poma L, Jouret F, Detry O. Effect of the Combination of Everolimus and Mesenchymal Stromal Cells on Regulatory T Cells Levels and in a Liver Transplant Rejection Model in Rats. *Front Immunol* 2022; **13**: 877953 [PMID: 35757737 DOI: 10.3389/fimmu.2022.877953]

9 **Gonzalez-Pujana A**, Igartua M, Santos-Vizcaino E, Hernandez RM. Mesenchymal stromal cell based therapies for the treatment of immune disorders: recent milestones and future challenges. *Expert Opin Drug Deliv* 2020; **17**: 189-200 [PMID: 31918562 DOI: 10.1080/17425247.2020.1714587]

10 **Meenakshi Sundaram R**, Kadapakkam Nandabalan S, Rupert S, Srinivasan P, Sankar P, Patra B, Verma RS, Vennila R, Sathyanesan J, Rajagopal S. Differential immunomodulation of human mesenchymal stromal cells from various sources in an inflammation mimetic milieu. *Cytotherapy* 2022; **24**: 110-123 [PMID: 34740526 DOI: 10.1016/j.jcyt.2021.09.005]

11 **Lim JY**, Kim BS, Ryu DB, Kim TW, Park G, Min CK. The therapeutic efficacy of mesenchymal stromal cells on experimental colitis was improved by the IFN-γ and poly(I:C) priming through promoting the expression of indoleamine 2,3-dioxygenase. *Stem Cell Res Ther* 2021; **12**: 37 [PMID: 33413597 DOI: 10.1186/s13287-020-02087-7]

12 **Sun L**, Wang J, Wang Q, He Z, Sun T, Yao Y, Wang W, Shen P. Pretreatment of umbilical cord derived MSCs with IFN-γ and TNF-α enhances the tumor-suppressive effect on acute myeloid leukemia. *Biochem Pharmacol* 2022; **199**: 115007 [PMID: 35307345 DOI: 10.1016/j.bcp.2022.115007]

13 **Corbett JM**, Hawthorne I, Dunbar H, Coulter I, Chonghaile MN, Flynn CM, English K. Cyclosporine A and IFNγ licencing enhances human mesenchymal stromal cell potency in a humanised mouse model of acute graft versus host disease. *Stem Cell Res Ther* 2021; **12**: 238 [PMID: 33853687 DOI: 10.1186/s13287-021-02309-6]

14 **Deng J**, Li D, Huang X, Li W, Zhao F, Gu C, Shen L, Cao S, Ren Z, Zuo Z, Deng J, Yu S. Interferon-γ enhances the immunosuppressive ability of canine bone marrow-derived mesenchymal stem cells by activating the TLR3-dependent IDO/kynurenine pathway. *Mol Biol Rep* 2022; **49**: 8337-8347 [PMID: 35690960 DOI: 10.1007/s11033-022-07648-y]

15 **Favre D**, Mold J, Hunt PW, Kanwar B, Loke P, Seu L, Barbour JD, Lowe MM, Jayawardene A, Aweeka F, Huang Y, Douek DC, Brenchley JM, Martin JN, Hecht FM, Deeks SG, McCune JM. Tryptophan catabolism by indoleamine 2,3-dioxygenase 1 alters the balance of TH17 to regulatory T cells in HIV disease. *Sci Transl Med* 2010; **2**: 32ra36 [PMID: 20484731 DOI: 10.1126/scitranslmed.3000632]

16   **Matteoli G**, Mazzini E, Iliev ID, Mileti E, Fallarino F, Puccetti P, Chieppa M, Rescigno M. Gut CD103+ dendritic cells express indoleamine 2,3-dioxygenase which influences T regulatory/T effector cell balance and oral tolerance induction. *Gut* 2010; **59**: 595-604 [PMID: 20427394 DOI: 10.1136/gut.2009.185108]

17   **Mebarki M**, Iglicki N, Marigny C, Abadie C, Nicolet C, Churlaud G, Maheux C, Boucher H, Monsel A, Menasché P, Larghero J, Faivre L, Cras A. Development of a human umbilical cord-derived mesenchymal stromal cell-based advanced therapy medicinal product to treat immune and/or inflammatory diseases. *Stem Cell Res Ther* 2021; **12**: 571 [PMID: 34774107 DOI: 10.1186/s13287-021-02637-7]

18   **Chen X**, Wu Y, Wang Y, Chen L, Zheng W, Zhou S, Xu H, Li Y, Yuan L, Xiang C. Human menstrual blood-derived stem cells mitigate bleomycin-induced pulmonary fibrosis through anti-apoptosis and anti-inflammatory effects. *Stem Cell Res Ther* 2020; **11**: 477 [PMID: 33176882 DOI: 10.1186/s13287-020-01926-x]

19   **Xu X**, Jiang W, Chen L, Xu Z, Zhang Q, Zhu M, Ye P, Li H, Yu L, Zhou X, Zhou C, Chen X, Zheng X, Xu K, Cai H, Zheng S, Wu X, Li D, Luo Q, Wang Y, Qu J, Li Y, Zheng W, Jiang Y, Tang L, Xiang C, Li L. Evaluation of the safety and efficacy of using human menstrual blood-derived mesenchymal stromal cells in treating severe and critically ill COVID-19 patients: An exploratory clinical trial. *Clin Transl Med* 2021; **11**: e297 [PMID: 33634996 DOI: 10.1002/ctm2.297]

20   **Zhang S**, Chang Q, Li P, Tong X, Feng Y, Hao X, Zhang X, Yuan Z, Tan J. Concentrated small extracellular vesicles from menstrual blood-derived stromal cells improve intrauterine adhesion, a pre-clinical study in a rat model. *Nanoscale* 2021; **13**: 7334-7347 [PMID: 33889891 DOI: 10.1039/d0nr08942g]

21   **Dominici M**, Le Blanc K, Mueller I, Slaper-Cortenbach I, Marini F, Krause D, Deans R, Keating A, Prockop Dj, Horwitz E. Minimal criteria for defining multipotent mesenchymal stromal cells. The International Society for Cellular Therapy position statement. *Cytotherapy* 2006; **8**: 315-317 [PMID: 16923606 DOI: 10.1080/14653240600855905]

22   **Rockenfeller P**, Koska M, Pietrocola F, Minois N, Knittelfelder O, Sica V, Franz J, Carmona-Gutierrez D, Kroemer G, Madeo F. Phosphatidylethanolamine positively regulates autophagy and longevity. *Cell Death Differ* 2015; **22**: 499-508 [PMID: 25571976 DOI: 10.1038/cdd.2014.219]

23   **Li W**, Luo LX, Zhou QQ, Gong HB, Fu YY, Yan CY, Li E, Sun J, Luo Z, Ding ZJ, Zhang QY, Mu HL, Cao YF, Ouyang SH, Kurihara H, Li YF, Sun WY, Li M, He RR. Phospholipid peroxidation inhibits autophagy *via* stimulating the delipidation of oxidized LC3-PE. *Redox Biol* 2022; **55**: 102421 [PMID: 35964342 DOI: 10.1016/j.redox.2022.102421]

24   **Zhou J**, Li XY, Liu YJ, Feng J, Wu Y, Shen HM, Lu GD. Full-coverage regulations of autophagy by ROS: from induction to maturation. *Autophagy* 2022; **18**: 1240-1255 [PMID: 34662529 DOI: 10.1080/15548627.2021.1984656]

25   **Xu Y**, Wan W. Acetylation in the regulation of autophagy. *Autophagy* 2023; **19**: 379-387 [PMID: 35435793 DOI: 10.1080/15548627.2022.2062112]

26   **Lynch K**, Treacy O, Chen X, Murphy N, Lohan P, Islam MN, Donohoe E, Griffin MD, Watson L, McLoughlin S, O'Malley G, Ryan AE, Ritter T. TGF-β1-Licensed Murine MSCs Show Superior Therapeutic Efficacy in Modulating Corneal Allograft Immune Rejection In Vivo. *Mol Ther* 2020; **28**: 2023-2043 [PMID: 32531237 DOI: 10.1016/j.ymthe.2020.05.023]

27   **Bai M**, Zhang L, Fu B, Bai J, Zhang Y, Cai G, Bai X, Feng Z, Sun S, Chen X. IL-17A improves the efficacy of mesenchymal stem cells in ischemic-reperfusion renal injury by increasing Treg percentages by the COX-2/PGE2 pathway. *Kidney Int* 2018; **93**: 814-825 [PMID: 29132705 DOI: 10.1016/j.kint.2017.08.030]

28   **de Pedro MÁ**, Gómez-Serrano M, Marinaro F, López E, Pulido M, Preußer C, Pogge von Strandmann E, Sánchez-Margallo FM, Álvarez V, Casado JG. IFN-Gamma and TNF-Alpha as a Priming Strategy to Enhance the Immunomodulatory Capacity of Secretomes from Menstrual Blood-Derived Stromal Cells. *Int J Mol Sci* 2021; **22** [PMID: 34830067 DOI: 10.3390/ijms222212177]

29   **Gong C**, Chang L, Sun X, Qi Y, Huang R, Chen K, Wang B, Kang L, Wang L, Xu B. Infusion of two-dose mesenchymal stem cells is more effective than a single dose in a dilated cardiomyopathy rat model by upregulating indoleamine 2,3-dioxygenase expression. *Stem Cell Res Ther* 2022; **13**: 409 [PMID: 35962420 DOI: 10.1186/s13287-022-03101-w]

30   **Li Y**, Hao J, Hu Z, Yang YG, Zhou Q, Sun L, Wu J. Current status of clinical trials assessing mesenchymal stem cell therapy for graft versus host disease: a systematic review. *Stem Cell Res Ther* 2022; **13**: 93 [PMID: 35246235 DOI: 10.1186/s13287-022-02751-0]

31   **Grégoire C**, Ritacco C, Hannon M, Seidel L, Delens L, Belle L, Dubois S, Vériter S, Lechanteur C, Briquet A, Servais S, Ehx G, Beguin Y, Baron F. Comparison of Mesenchymal Stromal Cells From Different Origins for the Treatment of Graft-vs.-Host-Disease in a Humanized Mouse Model. *Front Immunol* 2019; **10**: 619 [PMID: 31001253 DOI: 10.3389/fimmu.2019.00619]

32   **Yang SL**, Tan HX, Niu TT, Liu YK, Gu CJ, Li DJ, Li MQ, Wang HY. The IFN-γ-IDO1-kynureine pathway-induced autophagy in cervical cancer cell promotes phagocytosis of macrophage. *Int J Biol Sci* 2021; **17**: 339-352 [PMID: 33390854 DOI: 10.7150/ijbs.51241]

33   **Chaudhary K**, Shinde R, Liu H, Gnana-Prakasam JP, Veeranan-Karmegam R, Huang L, Ravishankar B, Bradley J, Kvirkvelia N, McMenamin M, Xiao W, Kleven D, Mellor AL, Madaio MP, McGaha TL. Amino acid metabolism inhibits antibody-driven kidney injury by inducing autophagy. *J Immunol* 2015; **194**: 5713-5724 [PMID: 25980011 DOI: 10.4049/jimmunol.1500277]

34   **Böttcher M**, Hofmann AD, Bruns H, Haibach M, Loschinski R, Saul D, Mackensen A, Le Blanc K, Jitschin R, Mougiakakos D. Mesenchymal Stromal Cells Disrupt mTOR-Signaling and Aerobic Glycolysis During T-Cell Activation. *Stem Cells* 2016; **34**: 516-521 [PMID: 26485560 DOI: 10.1002/stem.2234]

35   **Metz R**, Rust S, Duhadaway JB, Mautino MR, Munn DH, Vahanian NN, Link CJ, Prendergast GC. IDO inhibits a tryptophan sufficiency signal that stimulates mTOR: A novel IDO effector pathway targeted by D-1-methyl-tryptophan. *Oncoimmunology* 2012; **1**: 1460-1468 [PMID: 23264892 DOI: 10.4161/onci.21716]

36   **Sharma MD**, Pacholczyk R, Shi H, Berrong ZJ, Zakharia Y, Greco A, Chang CS, Eathiraj S, Kennedy E, Cash T, Bollag RJ, Kolhe R, Sadek R, McGaha TL, Rodriguez P, Mandula J, Blazar BR, Johnson TS, Munn DH. Inhibition of the BTK-IDO-mTOR axis promotes differentiation of monocyte-lineage dendritic cells and enhances anti-tumor T cell immunity. *Immunity* 2021; **54**: 2354-2371.e8 [PMID: 34614413 DOI: 10.1016/j.immuni.2021.09.005]

37   **Wu Y**, Chen X, Zhao Y, Wang Y, Li Y, Xiang C. Genome-wide DNA methylation and hydroxymethylation analysis reveal human menstrual blood-derived stem cells inhibit hepatocellular carcinoma growth through oncogenic pathway suppression *via* regulating 5-hmC in enhancer elements. *Stem Cell Res Ther* 2019; **10**: 151 [PMID: 31151404 DOI: 10.1186/s13287-019-1243-8]

38   **Ren HZ**, Xia SZ, Qin XQ, Hu AY, Wang JL. FOXO1 Alleviates Liver Ischemia-reperfusion Injury by Regulating the Th17/Treg Ratio through the AKT/Stat3/FOXO1 Pathway. *J Clin Transl Hepatol* 2022; **10**: 1138-1147 [PMID: 36381102 DOI: 10.14218/JCTH.2021.00551]

39   **Hu Y**, Zhan F, Wang Y, Wang D, Lu H, Wu C, Xia Y, Meng L, Zhang F, Wang X, Zhou S. The Ninj1/Dusp1 Axis Contributes to Liver Ischemia Reperfusion Injury by Regulating Macrophage Activation and Neutrophil Infiltration. *Cell Mol Gastroenterol Hepatol* 2023; **15**: 1071-1084 [PMID: 36731792 DOI: 10.1016/j.jcmgh.2023.01.008]

40   **Lu T**, Li Q, Lin W, Zhao X, Li F, Ji J, Zhang Y, Xu N. Gut Microbiota-Derived Glutamine Attenuates Liver Ischemia/Reperfusion Injury *via* Macrophage Metabolic Reprogramming. *Cell Mol Gastroenterol Hepatol* 2023; **15**: 1255-1275 [PMID: 36706918 DOI: 10.1016/j.jcmgh.2023.01.004]